TECHNIQUES AND ADAPTATION ALGORITHMS FOR DIRECT-SEQUENCE SPREAD-SPECTRUM CDMA SINGLE-USER DETECTION

by

Nevena Zečević

Thesis submitted to the Faculty of the
Virginia Polytechnic Institute and State University
in partial fulfillment of the requirements for the degree of

MASTER OF SCIENCE
in
Electrical Engineering

Approved:

Dr. Jeffrey H. Reed
(Chairman)

Dr. Brian D. Woerner

Dr. Dennis G. Sweeney

July 1996
Blacksburg, Virginia
Keywords: Spread Spectrum, CDMA, Receiver, Interference Rejection, Adaptation

Techniques and Adaptation Algorithms for Direct-Sequence Spread-Spectrum CDMA Single-User Detection

by

Nevena Zečević

Committee Chairman: Dr. Jeffrey H. Reed

Electrical Engineering

Abstract

The capacity of a *direct-sequence spread-spectrum code division multiple access (DSSS-CDMA)* system is limited by multiple access interference (MAI) and the near-far problem. There are two approaches to mitigating these problems: multiuser detection and single-user detection techniques. Multiuser detection techniques cancel the interference and enhance system capacity, but have large computational requirements and require the knowledge of MAI parameters. Single-user detection techniques require only the knowledge of the desired user's spreading code and timing, and have a complexity comparable to the conventional receiver.

This thesis reviews a wide range of DSSS-CDMA single-user detectors found in the literature. The receivers are explained with a common approach using an adaptive antenna array perspective and noting that single-user detectors exploit spectral redundancy, while adaptive arrays exploit spatial redundancy. Commonly used trained adaptation algorithms for single-user detection are first presented, and are followed by newly proposed blind adaptation algorithms. These new blind algorithms are *Griffiths' algorithm*, and the *linearly constrained constant modulus algorithm (LCCMA)*. Through simulation, a blindly-adapted single-user detector is shown to greatly outperform the conventional receiver in terms of bit-error-rate (BER) performance, and to perform almost as well as in

the case of trained adaptation. The receivers are shown to be near-far resistant, and are computationally attractive for a mobile receiver. Both receivers have good convergence properties and don't suffer from catastrophic failure.

Acknowledgements

I would like to express my gratitude to Dr. Jeffrey Reed for the opportunity to do exciting work under his guidance, and for his ideas, direction, comments and contribution to this thesis.

I wish to thank Dr. Ivan Howitt for his excellent suggestions and comments, very helpful in preparing the final draft of the report. I also appreciate the critical reviews provided by Dr. Woerner and Dr. Sweeney.

Many of my MPRG colleagues provided me with valuable help by discussing various technical issues, sharing their knowledge and answering my questions. I am most indebted to Milap Majmundar, Tom Biedka, Francis Dominique, Paul Petrus, Michael Buehrer, Joe Liberti, Volker Aue, Rong He, Rias Muhamed, and Nitin Mangalvedhe.

Abbreviations

AWGN	additive white Gaussian noise
BER	bit error rate
BPSK	binary phase shift keying
CDMA	code division multiple access
CHRT-LAR	chip-rate linear adaptive receiver
CM	constant modulus
CMA	constant modulus algorithm
CSFB-LAR	cyclically shifted filter bank linear adaptive receiver
CW-FS-LAR	complex-weight fractionally-spaced linear adaptive receiver
DD	decision directed
DOA	direction of arrival
DSO-LAR	data symbol oversampling linear adaptive receiver
DSSS	direct-sequence spread spectrum
EGID	eigenvector identification
FDMA	frequency division multiple access
FFT	fast Fourier transform
FRESH	frequency shift
FS-DFAR	fractionally-spaced decision-feedback adaptive receiver
FSR	Fourier series representation
GSC	generalized sidelobe canceller
ISI	intersymbol interference
LCCMA	linearly constrained constant modulus algorithm
LCL-FSR-SE	linear-conjugate-linear Fourier series representation sequence estimator
LMS	least mean square
LS	least squares

MAI	multiple access interference
MIMO	multi-input and multi-output
MMSE	minimum mean-squared error
MSE	mean-squared error
MSINR	maximum signal-to-interference-and-noise ratio
NLMS	normalized least mean square
RLS	recursive least squares
RW-FS-LAR	real-weight fractionally-spaced linear adaptive adaptive receiver
SDR	symmetric dimension reduction
SINR	signal-to-interference-and-noise ratio
SISO	single-input and single-output
SNOI	signal not of interest
SOI	signal of interest
TDAF	time-dependent adaptive filter
TDMA	time division multiple access

Contents

List of Figures

List of Tables

Chapter 1

Introduction

In cellular radio systems, *direct-sequence spread-spectrum code division multiple access (DSSS-CDMA)* promises great capacity improvements over standard multiple access techniques, namely frequency division multiple access (FDMA) and time division multiple access (TDMA). In DSSS-CDMA different users' signals share the same frequency band simultaneously in time, as opposed to FDMA, where users are assigned different frequency channels and are simultaneous in time, and TDMA, where users are assigned different time slots and share the same spectrum. With DSSS-CDMA each user is assigned a particular *spreading waveform*, a bit sequence chosen to be approximately orthogonal to the spreading waveforms of other users. The spreading waveform has a higher rate than the data signal which modulates it, and the modulated signal bandwidth is larger that that of the data signal, i.e., the spectrum is spread. The spreading waveform is also referred to as the *spreading code*, while its bits are called *chips*, and the ratio of the spread bandwidth to the data rate is the *processing gain.*

Unlike FDMA and TDMA, the capacity of a CDMA system tends not to be noise limited, but is limited by multiple access interference (MAI), which stems from the lack of orthogonality between the spreading waveforms of different users and is exasperated by the near-far problem. It is important to note that these limitations are not an inherent property of CDMA, but result from the use of the *conventional DSSS receiver* and its inability to exploit the structure of the MAI.

The conventional receiver consists of a filter matched to the desired user's spreading code and a decision device. It is the optimal demodulator for a DSSS signal

in additive white Gaussian noise (AWGN), and has the advantage of being simple and easy to implement. The fact that the conventional receiver views the MAI as AWGN and disregards its structure, and the fact that there is a large disparity in the received powers of different users' signals (i.e., the near-far problem), have provided motivation for the use of a large variety of signal processing techniques to enhance the capacity of CDMA systems. Among them, different receiver structures and interference canceling algorithms have been proposed, mainly concentrating on detecting all the users' signals at the same time, i.e., achieving *multiuser detection* [2], [3].

Multiuser detection techniques strive to approach the performance of the maximum likelihood sequence detector [4], which is the optimum multiuser receiver. The optimum receiver has a complexity which increases exponentially with the number of users, while the complexity of sub-optimum multiuser receivers is in most cases linear in the number of users.

Multiuser detection techniques require the knowledge of all the users' spreading codes and timings, the knowledge of all or some of the interferers' received powers, and the knowledge of channel parameters. These constraints have motivated the development of *single-user detection* techniques for DSSS-CDMA [5]–[14]. These receivers detect a single user's signal, and require only the knowledge of the desired user's spreading code and timing. While the multiuser receivers can be viewed as multi-input and multi-output (MIMO) structures, single-user detectors are single-input single-output (SISO) structures. They have a complexity which is independent of the number of users, much smaller than the complexity of the multiuser receivers, and comparable to the complexity of the conventional receiver. In fact, in some cases they have the same structure as the conventional receiver, the only difference being that the filter weights are not fixed, but adaptive.

Adaptive receivers performing single-user detection have great advantages over the conventional receiver. They perform despreading, interference rejection and in some cases act as a RAKE receiver, coherently combining multipath. They also provide near-far resistance, making the power control requirements much less stringent. Their adaptive nature makes it possible for them to handle time-varying system parameters such as varying channel characteristics and number of users. They achieve better bit error rates (BERs) and provide a larger capacity than the conventional receiver.

There are applications for which single-user receivers are far more suitable than

multiuser receivers. One such application is rejecting out-of-cell interference for cellular radio. While the information about the spreading codes of all the users in a cell is provided to the base station, the out-of-cell interferers' parameters may not be available. Single-user detectors can successfully reject interference without the knowledge of any interferer's spreading code. Also, the small complexity and computational requirements of these receivers make them far more suitable for the mobile or portable unit. The fact that the receiver doesn't require the knowledge of any other user's code implies higher security. Finally, adaptive receivers performing single-user detection can be used in ad-hoc networks, where users communicate with each other directly without a central base station. For this application the receivers do not have central power control or the knowledge of other users' spreading codes and due to weight/size constraints the receivers must be limited to a reasonable complexity.

This work discusses a wide range of DSSS-CDMA single-user detectors found in the literature (Chapter 2). They are classified as chip-rate and fractionally-spaced receivers, reduced- and optimum-complexity receivers, and linear and non-linear receivers. A contribution is made by putting the problem of single-user detection in a unifying perspective by noting that the receivers exploit the cyclostationarity inherent in the DSSS-CDMA signal, and by presenting the analogy between single-user detection, which exploits spectral redundancy, and beamforming, which exploits spatial redundancy. Both approaches give insight into the creation and analysis of different single-user detection techniques.

Since the single-user detectors presented are adaptive receivers, commonly used trained adaptation algorithms are presented (Chapter 3), namely the least-mean-square (LMS) algorithm, the normalized least-mean-square (NLMS) algorithm, and the recursive least-squares (RLS) algorithm. It is recognized that blind adaptation algorithms are more suitable, because they don't require a training sequence and because the transmission needn't be interrupted for retraining when there is a sudden and large change in the system. Three blind adaptation algorithms novel in the area of DSSS-CDMA single-user detection are derived to suit this application. They are the Griffiths' algorithm, the constant modulus algorithm (CMA), and the linearly constrained constant modulus algorithm (LCCMA). All three are commonly used to adapt antenna arrays for beamforming, and their application to single-user detection is an original contribution. The algorithms are shown to have complexities comparable

to those of the simpler trained adaptation algorithms, namely the LMS and the NLMS.

In Chapter 4, where simulation results are presented, it is shown that the CMA suffers from the problem of capturing an interferer instead of the desired user, due to the algorithm's inability to distinguish between different constant modulus signals. The Griffiths' algorithm and the LCCMA are shown to successfully detect the desired signal and approximately zero-out the MAI; i.e., both algorithms implement an approximate zero-forcing solution. The two blind algorithms are found to converge as fast as the NLMS, and they are shown not to suffer from catastrophic failure. Chapter 4 also investigates the BER performance of a blindly adapted single-user detector. A major capacity improvement over conventional detection is observed, and just a slight degradation relative to the trained adaptation case. The detector is also shown to be near-far resistant even for large disparities in the powers of the MAI.

Chapter 2

DSSS-CDMA Single-User Detection Techniques

This chapter presents a DSSS-CDMA system model and discusses various DSSS-CDMA single-user detectors. The detectors covered are the chip-rate linear adaptive receivers, the chip-rate linear adaptive receivers of reduced complexity and of optimum complexity, fractionally-spaced linear adaptive receivers, and non-linear fractionally-spaced decision-feedback adaptive receivers. The problem of single-user detection is put in a unifying perspective by noting that for the best performance the receiver exploits the cyclostationarity inherent in the DSSS-CDMA signal, and by showing the analogy between single-user detection and beamforming. This perspective gives insight into the creation and analysis of different single-user detection techniques.

2.1 System Description

We consider an asynchronous DSSS-CDMA system with K users. Each user's data signal is spread and binary-phase-shift keying (BPSK) modulated, and all the resulting signals are simultaneously transmitted over an AWGN channel. The complex bandpass representation of the kth user's transmitted signal is given by

$$x_k(t) = \sqrt{P_{tk}} \sum_{m=-\infty}^{\infty} d_k(m) s_k(t - mT - \tau_k) e^{j[\omega_k(t-\tau_k)+\theta_k]}, \qquad (2.1)$$

where P_{tk} is the kth user's transmitted signal power; $d_k(m)$ is the kth user's data symbol at the mth symbol interval, $d_k(m) \in \{-1, +1\}$; $s_k(t)$ is the kth users'

spreading waveform; T is the symbol period; and $k = 1, 2, \ldots, K$. The kth user's delay, $\tau_k \in [0, T]$, is chosen to be an integer multiple of the sampling period T_s, which is in turn equal to a fraction of the chip period, T_c. The processing gain is N. Therefore, $\tau_k = l_k \cdot T_s$, l_k is a uniformly distributed discrete random variable, $l_k \in \{0, 1, \ldots, pN - 1\}$, $T_s = T_c/p$, where p is an integer, and $T_c = T/N$. The kth user's carrier frequency is $\omega_k = \omega_c + \Delta\omega_k$, where ω_c is the nominal carrier frequency, and $\Delta\omega_k$ is the carrier frequency offset for user k. The carrier phase is denoted as θ_k, and is uniformly distributed over the interval $[0, 2\pi]$.

The kth user's spreading waveform is given by

$$s_k(t) = \sum_{n=0}^{N-1} s_{kn} \Pi_{T_c}(t - nT_c), \qquad 0 \le t \le T, \tag{2.2}$$

where $s_k(t) = 0$ for $t \notin [0, T]$. The nth chip of the kth user's spreading code is denoted as s_{kn}, and $\Pi_{T_c}(t)$ is a rectangular pulse of duration T_c. The kth user's spreading code can be represented in the form of a vector given by

$$\mathbf{S}_k = \begin{bmatrix} s_{k0} & s_{k1} & \cdots & s_{k(N-1)} \end{bmatrix}^T. \tag{2.3}$$

For a spreading waveform defined by (2.2), *code-on-pulse* modulation or *modulation-on-symbol* is employed, i.e., the spreading code of each user repeats with a period equal to the symbol interval T.

It is assumed that for the desired user $k = 1$, $\tau_1 = 0$, $\Delta\omega_1 = 0$, and $\theta_1 = 0$, i.e., the receiver is perfectly synchronized with the desired user's signal. After downconversion to baseband, the received signal can be written as

$$r(t) = r_1(t) + \sum_{k=2}^{K} r_k(t) + n(t), \tag{2.4}$$

where $r_k(t)$ is the kth user's received and downconverted signal,

$$r_k(t) = \sqrt{P_{rk}} \sum_{m=-\infty}^{\infty} d_k(m) s_k(t - mT - \tau_k) e^{j[\Delta\omega_k(t-\tau_k) - \omega_c\tau_k + \theta_k]}, \tag{2.5}$$

its received power denoted as P_{rk} ($P_{r1} = 1$ is assumed), and $n(t)$ is complex white Gaussian noise,

$$n(t) = n_r(t) + j \cdot n_i(t). \tag{2.6}$$

The two real baseband white Gaussian noise processes, denoted as $n_r(t)$ and $n_i(t)$, have double-sided power spectral densities of N_0.

The presented system model is similar to the ones found in [5]–[10], [12], [13], [17]–[19].

Figure 2.1: Conventional receiver

2.2 Chip-Rate Linear Adaptive Receivers

Chip-rate linear adaptive receivers performing single-user detection are derived from the conventional receiver, which can be implemented as a chip-matched filter followed by a transversal matched filter, as shown in Figure 2.1.

The received signal $r(t)$ is passed through a filter matched to the chip waveform, i.e., a chip-matched filter. In case of a digital implementation of the chip-matched filter in the form of a linear transversal filter, the received signal $r(t)$ is first sampled at a rate equal to a multiple of the chip rate. The sampling interval is $T_s = T_c/p$, where T_c is the chip interval, and p is an integer, as defined in the previous section. The output of the chip-matched filter $r_c(t)$ is sampled at the chip rate $1/T_c$, and then input to an N-tap linear transversal filter whose weights are fixed and form a vector equal to the desired user's spreading code $\mathbf{s}_1$. The output of the transversal matched filter is sampled at the data rate $1/T$ to obtain an estimate for the desired user's mth data symbol $y_1(m)$, and subsequently the hard decision $\hat{d}_1(m)$.

A chip-rate linear adaptive receiver for CDMA single-user detection was proposed by Madhow and Honig in [5]–[7] and Agee in [8]. This *N-tap chip-rate linear adaptive receiver (N-tap CHRT-LAR)*, referred to as the N-tap MMSE detector by Madhow and Honig, and the optimal linear despreader by Agee, has the same structure as the previously described conventional receiver. The only difference is that the weights of the chip-spaced linear transversal filter are not fixed, but adapted according to the *minimum mean-squared error (MMSE)* criterion (Figure 2.2).

Just as the conventional receiver, the N-tap CHRT-LAR performs symbol-by-symbol detection. Since code-on-pulse modulation is employed, the adaptive chip-spaced linear transversal filter corresponds to one data symbol in length.

The samples corresponding to the mth data symbol form a chip-spaced received

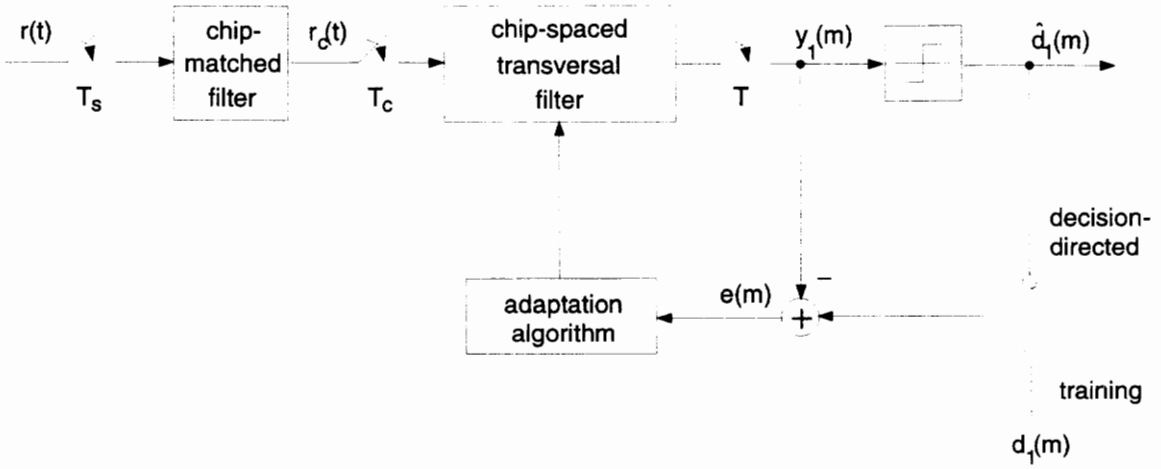

Figure 2.2: N-tap chip-rate linear adaptive receiver (N-tap CHRT-LAR)

signal vector given by

$$\mathbf{r}_c(m) = \left[\begin{array}{cccc} r_{c0}(m) & r_{c1}(m) & \cdots & r_{c(N-1)}(m) \end{array} \right]^T, \tag{2.7}$$

while the filter weights form a weight vector given by

$$\mathbf{w} = \left[\begin{array}{cccc} w_0 & w_1 & \cdots & w_{N-1} \end{array} \right]^T. \tag{2.8}$$

The filtering operation is modeled by

$$y_1(m) = \mathbf{w}^T \mathbf{r}_c(m), \tag{2.9}$$

where $[\cdot]^T$ denotes the matrix transpose operation, and the weight vector $\mathbf{w}$ is chosen to minimize the mean-squared error

$$MSE = \mathrm{E}[|e(m)|^2]. \tag{2.10}$$

The error signal $e(m)$ is formed as the difference between a reference signal and the output of the transversal filter, i.e., the estimate. The best choice for the reference signal is the true data symbol $d_1(m)$. During initial adaptation, a training sequence is used and the error signal is given by

$$e(m) = d_1(m) - y_1(m). \tag{2.11}$$

After the adaptation algorithm converges, decision-directed adaptation is employed, and the reference signal is the estimated data symbol, i.e., the hard decision $\hat{d}_1(m) = \text{sgn}\{\text{Re}[y_1(m)]\}$. The error signal is now given by

$$e(m) = \hat{d}_1(m) - y_1(m). \tag{2.12}$$

The N-tap CHRT-LAR performs much better than the conventional receiver, in terms of BER and near-far resistance, as shown by Madhow and Honig in [5]–[7] and Agee in [8]. The receiver mitigates the near-far problem of conventional detection, and alleviates the need for stringent power control. There is a price to be paid for this improvement, however, and that is the increased complexity, which results from the adaptive nature of the receiver.

The adaptive receiver's computational requirements depend on the choice of the adaptation algorithm and the number of adaptive weights, i.e., the processing gain N. A large processing gain will result in large computational requirements, a slow convergence rate, and a potentially large filter misadjustment.

2.2.1 Complexity Reduction of the Chip-Rate Linear Adaptive Receivers

Two adaptive receivers for CDMA single-user detection that have a smaller number of adaptive weights than the N-tap CHRT-LAR are proposed by Madhow and Honig in [5]–[7]. They are the *data symbol oversampling linear adaptive receiver (DSO-LAR)*, referred to as the oversampling scheme by Madhow and Honig, and the *cyclically shifted filter bank linear adaptive receiver (CSFB-LAR).*

For both reduced-complexity adaptive receivers, the operations of despreading and interference rejection are separated. The received signal is first despread, and only then processed adaptively. Just as in the case of conventional detection, the despreading is performed by a chip-matched filter followed by a transversal matched filter.

In the case of the DSO-LAR, which is shown in Figure 2.3, the output of the transversal matched filter is sampled D times per symbol, the sampling interval being $T_D = T/D$. The despread signal samples are input to a linear transversal filter with tap spacing T_D and weights that are adapted according to the MMSE criterion. The

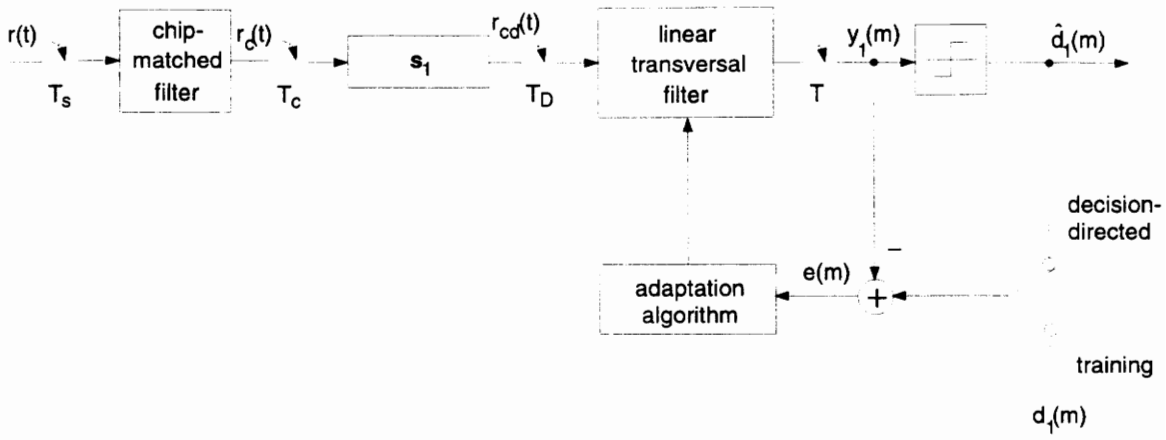

Figure 2.3: Data symbol oversampling linear adaptive receiver (DSO-LAR)

output of the adaptive filter is sampled at the data rate $1/T$ to obtain the estimate for the desired user's mth data symbol $y_1(m)$.

The CSFB-LAR, which is shown in Figure 2.4, consists of a chip-matched filter and a bank of D N-tap linear transversal filters. The first filter in the bank is the transversal matched filter for the desired user, and its output is the despread received signal. The other $D-1$ filters are cyclically shifted versions of the matched filter, the successive shifts being spaced by T_D. The outputs of the filter bank are sampled at the data rate $1/T$, and linearly and adaptively combined to obtain the estimate $y_1(m)$. The weights of the linear combiner are adapted according to the MMSE criterion.

The estimate produced by the two reduced-complexity adaptive receivers is given by

$$y_1(m) = \mathbf{w}^T \mathbf{r}_{cd}(m). \tag{2.13}$$

In the case of the DSO-LAR, $\mathbf{w}$ is the adaptive filter weight vector, given by

$$\mathbf{w} = \begin{bmatrix} w_0 & w_1 & \cdots & w_{D-1} \end{bmatrix}^T, \tag{2.14}$$

and $\mathbf{r}_{cd}(m)$ is the chip-spaced despread signal vector, given by

$$\mathbf{r}_{cd}(m) = \begin{bmatrix} r_{cd0}(m) & r_{cd1}(m) & \cdots & r_{cd(D-1)}(m) \end{bmatrix}^T. \tag{2.15}$$

In the case of the CSFB-LAR, $\mathbf{w}$ is the adaptive linear combiner weight vector, given by (2.14), and $\mathbf{r}_{cd}$ is the vector of the filter bank output samples, given by (2.15).

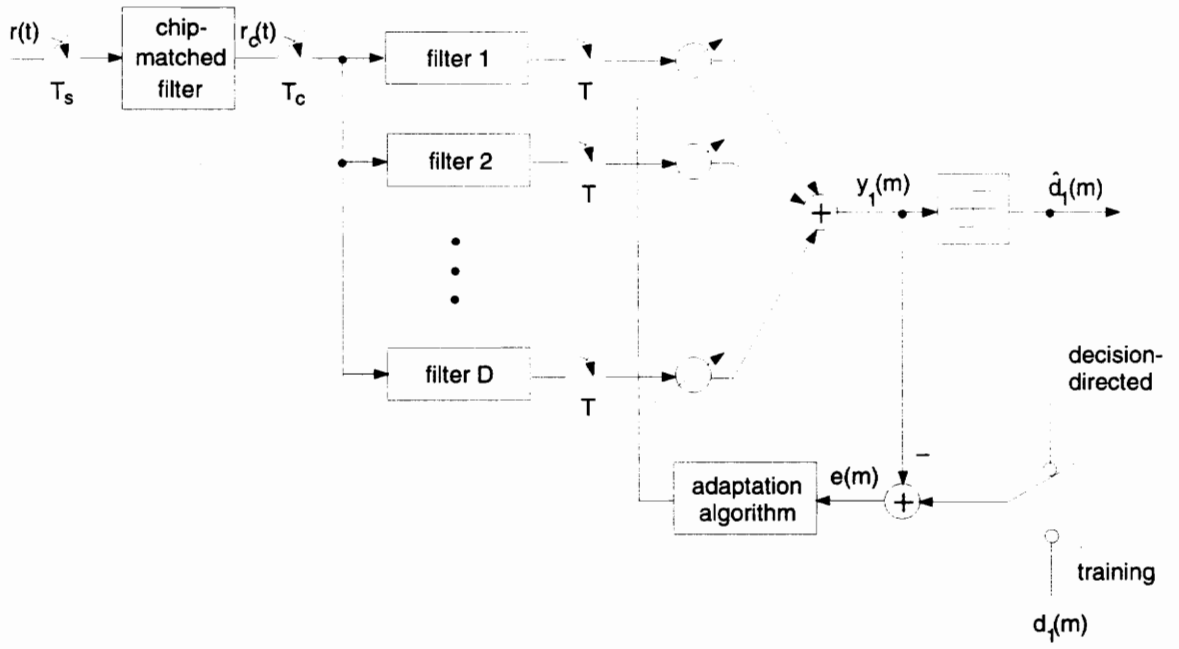

Figure 2.4: Cyclically shifted filter bank linear adaptive receiver (CSFB-LAR)

The number of adaptive components for the DSO-LAR and the CSFB-LAR, D, is chosen to be smaller than the processing gain N, for reduced complexity. While it can be argued that the structure of the two described adaptive receivers is more complex than that of the N-tap CHRT-LAR in terms of the number of fixed components, the complexity is certainly reduced in terms of the number of adaptive components, which results in reduced computational requirements.

Unfortunately, reduced complexity also means a degradation in performance. While the N-tap CHRT-LAR has N degrees of freedom and is, therefore, capable of rejecting up to $N-1$ synchronous interferers, or $(N-1)/2$ asynchronous ones (this is justified in [7] by investigating the receiver's near-far resistance), the two reduced-complexity adaptive receivers have a smaller number of degrees of freedom, equal to D. As explained in [5], assuming that the desired user's spreading code has good autocorrelation properties, the weight vectors of the D filters in the CSFB will be approximately orthogonal to each other, and will form a basis for a D-dimensional subspace. If this subspace contains the subspace spanned by the desired user's spreading code and the spreading codes of $D-1$ interferers, these interferers can be rejected.

Therefore, the CSFB-LAR can reject up to $D-1$ synchronous interferers, or $(D-1)/2$ asynchronous interferers. In the case of the DSO-LAR, a desired user's data symbol adjacent to the one being detected causes interference because the transient response of the matched filter overlaps with the next symbol. This causes the performance of the DSO-LAR to be worse than that of the CSFB-LAR in a synchronous system. In the asynchronous system case, the DSO-LAR can reject up to only $(D-1)/3$ interferers, since up to three interferer's data symbols corrupt the data symbol being detected [7]. In cases of both the N-tap CHRT-LAR and the CSFB-LAR in an asynchronous system, only two interferer's data symbols interfere with the detected data symbol, and there is no self-interference.

2.2.2 Optimum Complexity Reduction

The question of whether there exists a reduced-complexity adaptive receiver which achieves the same performance as the N-tap CHRT-LAR was answered by Ström and Miller in [9].

Ström and Miller show that the complexity of the N-tap CHRT-LAR, which is proportional to the dimension of the received vector $\mathbf{r}_c$ defined in (2.7), can be reduced by multiplying the received vector by $\mathbf{V}^*$, where $\mathbf{V}$ is a full rank matrix, and $[\cdot]^*$ denotes the conjugate operation. The resulting vector $\mathbf{V}^*\mathbf{r}_c$ has to be of a smaller dimension than $\mathbf{r}_c$, just as $\mathbf{r}_{cd}$ defined in (2.15) has a dimension D, smaller than N. The matrix $\mathbf{V}$ is *optimum* if the linear adaptive receiver that uses $\mathbf{V}^*\mathbf{r}_c$ as the input to the adaptive filter has the same BER as the receiver that uses $\mathbf{r}_c$, i.e., the N-tap CHRT-LAR. Ström and Miller show that this will be true if $\mathbf{V}^*\mathbf{V} = \mathbf{I}$, where $\mathbf{I}$ is the identity matrix of corresponding dimensions, and if the signal subspace is a subset of, or equal to, the space spanned by the columns of $\mathbf{V}$. It should be noted that, for $\mathbf{V}$ to be a complexity reduction transform, the number of interferers, that the signal subspace dimension depends on, needs to be smaller than N.

To compute the *optimum complexity reduction transform*, the knowledge of the signal subspace is required, which means that the knowledge of the propagation delays and spreading codes of all the users is required [9]. Since the basic assumption for single-user detection is that no interferer's parameters are known, it can be concluded that optimum complexity reduction cannot be achieved.

However, different complexity reduction schemes can be employed, and Ström and

Miller provide a performance measure in the form of a formula for the BER for a given scheme. They also propose two new reduction schemes, namely the *symmetric dimension reduction (SDR)* scheme, and the *eigenvector identification (EGID)* scheme. The descriptions for the reduction schemes can be found in [9].

2.3 Fractionally-Spaced Adaptive Receivers

Fractionally-spaced adaptive receivers performing single-user detection have a structure very similar to that of fractionally-spaced equalizers. While the equalizers reject intersymbol interference (ISI), the adaptive receivers do much more, including despreading the desired user's signal, rejecting MAI, combining multipath as RAKE receivers, and rejecting ISI. It is well known that fractionally-spaced equalizers perform better than their symbol-spaced counterparts, as shown by Gitlin and Weinstein in [20]. By analogy, fractionally-spaced adaptive receivers are expected to perform better than chip-spaced adaptive receivers and of course the conventional detector.

There are a variety of fractionally-spaced adaptive receivers used for CDMA single-user detection. They are classified as the *fractionally-spaced linear adaptive receivers* and the *non-linear fractionally-spaced decision-feedback adaptive receivers.*

2.3.1 Fractionally-Spaced Linear Adaptive Receivers and the Unifying Perspective for DSSS-CDMA Signal Detection

Fractionally-spaced linear adaptive receivers have a structure similar to the conventional receiver form that uses a fixed transversal filter to despread the signal. The *complex-weight fractionally-spaced linear adaptive receiver (CW-FS-LAR)* is obtained by making the transversal filter adaptive, and employing the MMSE adaptation criterion. Such a structure was proposed by Monogioudis et al. in [10], [11], where it was referred to as the linear fractionally-spaced equalizer, and Rapajić and Vučetić in [12], where it was referred to as the adaptive linear receiver.

The CW-FS-LAR is shown in Figure 2.5. The received signal $r(t)$ is sampled p times per chip, the sampling interval being $T_s = T_c/p$. The adaptive filter is at least Np taps long, i.e., at least one whole sampled spread data symbol is contained in

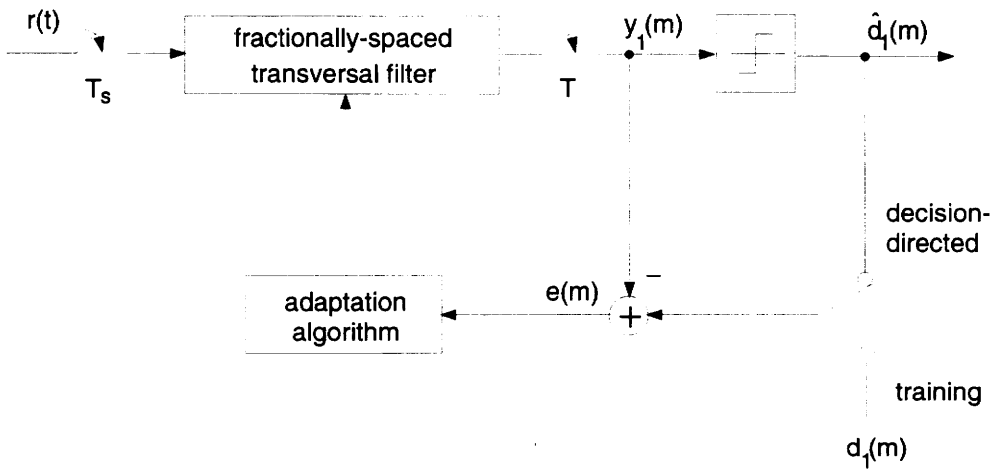

Figure 2.5: Complex-weight fractionally-spaced linear adaptive receiver (CW-FS-LAR)

the filter. The filter output is sampled at the data rate $1/T$ to obtain the estimate for the desired user's mth data symbol $y_1(m)$. The adaptation algorithm is chosen to minimize the MSE, and it operates either in the training adaptation mode, or the decision-directed adaptation mode.

Fractionally-spaced linear adaptive receivers that exploit the *spectral correlation* inherent to DSSS modulation were proposed by Aue and Reed in [13] and Holley and Reed in [15]. These single-user detection techniques recognize the fact that a DSSS signal is a cyclostationary process, which means that its statistics (i.e., its mean and autocorrelation function) can be represented as a generalized Fourier series. The frequencies for which the Fourier coefficients exist are called *cycle frequencies*, or *periodicities*. The signal is said to exhibit the spectral correlation property because of the correlation between its cycle-frequency-shifted versions.

DSSS signals have three fundamental statistical periodicities, namely the chip rate, the data rate, and the code repetition rate [13]–[15]. Other periodicities are formed from the harmonics of the fundamental periodicities. As shown in [15], when the chip rate, the data rate, and the code repetition rate are integrally related (e.g., in case of code-on-pulse modulation), there is a single fundamental periodicity. The fundamental periodicity is equal to the code repetition rate, and there is a significant degree of spectral correlation in the transmitted first null-to-null bandwidth of the

signal. To exploit the spectral correlation, a receiver should be an implementation of the *time-dependent adaptive filter (TDAF)*. The TDAF is a linear periodically time-variant filter that seeks to adaptively combine the correlated portions of the signal spectrum, and it is described in more detail in Section 2.4.

Aue and Reed derive a fractionally-spaced linear adaptive receiver that exploits the spectral correlation of DSSS signals by showing that the TDAF can be implemented as a fractionally-spaced adaptive linear transversal filter [13], [14]. They refer to it as the reduced linear-conjugate-linear Fourier series representation sequence estimator (reduced LCL-FSR-SE). The receiver performs LCL filtering, which is optimal for complex cyclostationary signals [22]. It consists of two complex-weight fractionally-spaced adaptive linear transversal filters, which filter in parallel the received complex signal and its conjugate. The two filter outputs are added to obtain the estimate $y_1(m)$. Aue and Reed reduce the complexity of the receiver by modifying it to adapt based only on the real portion of the estimate, since the real portion is what the hard decision is based on. For BPSK modulation the imaginary axis is the decision boundary and the hard decision is obtained as $\hat{d}_1(m) = \text{sgn}\{\text{Re}[y_1(m)]\}$.

The resulting *real-weight fractionally-spaced linear adaptive receiver (RW-FS-LAR)*, referred to as the optimum time-dependent DSSS detector in [13], is shown in Figure 2.6. It consists of two real-weight adaptive linear transversal filters, which filter the real and the imaginary portion of the received signal. The received signal is sampled at the rate $1/T_s$, and both filters are fractionally-spaced. The filter outputs are added, and the summed output is sampled at the data rate to obtain the estimate $y_1(m)$. The filters are adapted according to the MMSE criterion.

Both the CW-FS-LAR and the RW-FS-LAR achieve substantial performance improvement over the conventional receiver [10]–[14]. The two receivers are near-far resistant, and they coherently combine multipath, acting as RAKE receivers. The length of the fractionally-spaced adaptive linear transversal filters (i.e., the number of taps) and the sampling interval (i.e., the tap spacing) should be chosen according to the expected multipath delays and coherence bandwidth [14].

Another fractionally-spaced linear adaptive receiver that performs time-dependent adaptive filtering was proposed by Holley and Reed in [15]. It is a Fast Fourier transform (FFT) implementation of the TDAF, which performs waveform estimation, rather than signal detection. The full description of this receiver can be found in [15].

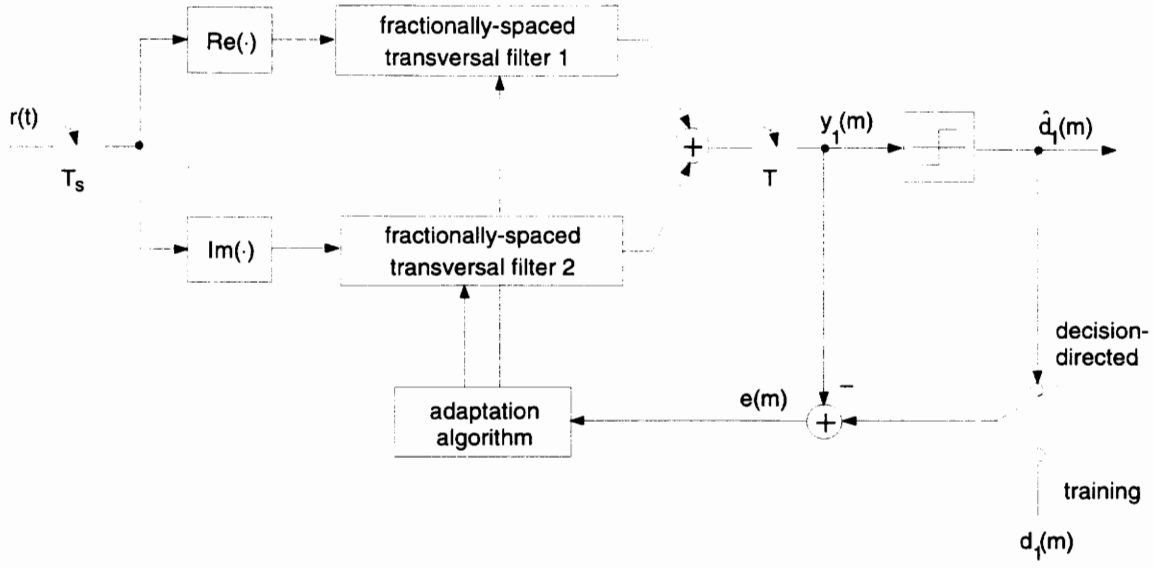

Figure 2.6: Real-weight fractionally-spaced linear adaptive receiver (RW-FS-LAR)

By recognizing the fact that DSSS signals are cyclostationary and exhibit the property of spectral correlation, the problem of DSSS-CDMA single-user detection is put in a unifying perspective. To exploit the spectral correlation, a receiver needs to be an implementation of the TDAF (this is explained in more depth in Section 2.4). All receiver structures that adaptively process the received signal without first despreading it are implementations of the TDAF, or their modifications. The difference between different structures is in how much of the spectral correlation they exploit. In the case of the RW-FS-LAR and the CW-FS-LAR (Figures 2.6 and 2.5), the former performs the LCL filtering and the latter doesn't, thus not fully exploiting the spectral correlation. The N-tap CHRT-LAR (Figure 2.2) can be viewed as a modification of the CW-FS-LAR (Figure 2.5). The signal input to the adaptive filter is sampled once instead of multiple times per chip, which still makes use of some of the spectral correlation (ideally, the sampling rate should be at least twice per chip [14]). In the case of receivers that first despread the received signal, however, the spectral correlation due to the DSSS signal's code repetition is lost and the adaptive receiver structure cannot exploit it.

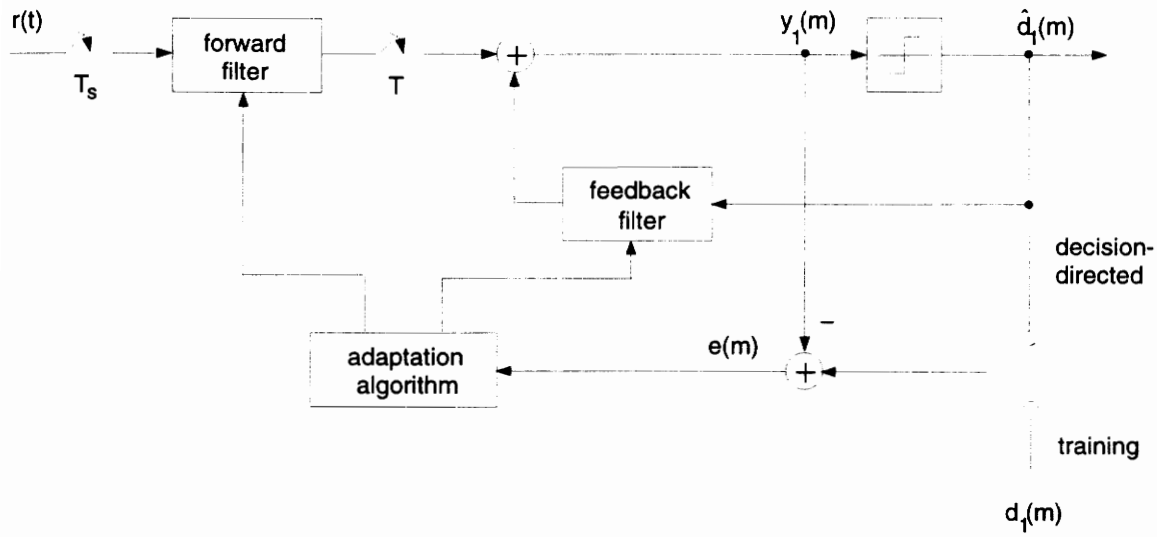

Figure 2.7: Fractionally-spaced decision-feedback adaptive receiver (FS-DFAR)

2.3.2 Non-Linear Fractionally-Spaced Decision-Feedback Adaptive Receivers

Non-linear fractionally-spaced decision-feedback adaptive receivers consist of a fractionally-spaced forward filter which is similar to the CW-FS-LAR, and a symbol-spaced feedback filter which feeds back the past data decisions. The non-linearity in the filter arises because of the quantization effect introduced in the decision making process. The basic structure is proposed by Monogioudis et al. in [11] and by Rapajić and Vučetić in [12]. The *fractionally-spaced decision-feedback adaptive receiver (FS-DFAR)* is shown in Figure 2.7, and is referred to as the fractionally-spaced decision-feedback equalizer in [11] and as the adaptive decision-feedback receiver in [12].

The FS-DFAR is more complex than its linear counterpart, the CW-FS-LAR. It is also more difficult to adapt, since the convergence of the adaptation algorithm is more sensitive to the choice of the step size (defined in Chapter 3). However, as shown in [11], in the presence of multipath it achieves better performance than the CW-FS-LAR. It is also shown it performs better than a RAKE receiver, coherently combining multipath while rejecting the MAI. In an AWGN channel, the FS-DFAR performs approximately the same as the CW-FS-LAR, as shown in [12], which is expected, since the feedback filter helps only with the ISI rejection. The receiver is also shown to be near-far resistant [11].

Two other decision-feedback receiver structures were proposed by Abdulrahman et al. in [17]–[19]. One consists of a filter matched to the desired user's spreading waveform followed by a FS-DFAR. The resulting fractionally-spaced adaptive receiver performs the operations of despreading and interference rejection separately. The other structure consists of a lowpass filter followed by a FS-DFAR, and is fairly similar to the FS-DFAR alone.

2.4 More on the Unifying Perspective for DSSS-CDMA Signal Detection: The Analogy with Beamforming

In this section, the need for the receiver to be an implementation of the TDAF is explained in more detail. Also, an analogy between DSSS-CDMA single-user detection and adaptive beamforming using an antenna array is presented, both in the time and frequency domains.

As discussed in Section 2.3.1, a DSSS signal is a cyclostationary process and has the property of spectral correlation. Versions of the signal spectrum shifted in frequency by the cycle frequencies are correlated. This can easily be understood considering that the spread signal spectrum is a sum of scaled and frequency-shifted versions of the data spectrum [23]. A spreading waveform $s(t)$ that repeats with period T can be modeled as the response of a filter $h_s(t)$ to a sequence of impulses,

$$s(t) = h_s(t) * \sum_{n=-\infty}^{\infty} \delta(t - nT), \tag{2.16}$$

where $a(t) * b(t)$ denotes the convolution of two waveforms $a(t)$ and $b(t)$. The spread baseband signal is obtained by modulating the spreading waveform by the data signal $d(t)$, and is given by

$$x(t) = d(t) \cdot \left[h_s(t) * \sum_{n=-\infty}^{\infty} \delta(t - nT) \right]. \tag{2.17}$$

Assuming for simplicity that the data signal is deterministic, this can be written in the frequency domain as

$$X(f) = D(f) * \left[H_s(f) \cdot \frac{1}{T} \sum_{n=-\infty}^{\infty} \delta(f - \frac{n}{T}) \right], \tag{2.18}$$

or

$$X(f) = \frac{1}{T} \sum_{n=-\infty}^{\infty} H_s\left(\frac{n}{T}\right) D\left(f - \frac{n}{T}\right), \tag{2.19}$$

where $D\left(f - \frac{n}{T}\right)$ is the data spectrum shifted in frequency by a multiple of the data rate $1/T$.

To despread the signal, an operation equivalent to spreading is required. It involves frequency shifting, scaling and adding the data spectra to obtain the original data signal. This is performed by a TDAF, an adaptive implementation of a *FREquency-Shift (FRESH) filter*, which seeks to linearly and adaptively combine the correlated replicas of the spread signal in order to estimate the data and reject the MAI. The filter is time-dependent, with an impulse response that can be written as a generalized Fourier series, i.e., it is a linear multiply-periodically time-variant filter [22]. One possible implementation of the TDAF is the Fourier series representation TDAF (FSR TDAF), shown in Figure 2.8. It consists of a bank of frequency shifters, the shifts being equal to the cycle frequencies of the filtered signal, α_i $(i = 0, 1, \ldots, M-1)$, followed by a bank of time-independent adaptive filters. In case of a DSSS signal and code-on-pulse modulation, the cycle frequencies are multiples of the code repetition rate $1/T$, i.e., $\alpha_i = \frac{i}{T}$, for $i = 0, 1, \ldots, M-1$.

The way signal despreading is performed by exploiting spectral correlation is similar to the way an adaptive antenna array exploits spatial diversity when performing beamforming. The array detects a signal coming from a certain direction in space by adaptively combining the correlated signals received by the antenna elements. A DSSS-CDMA single-user receiver can be viewed as an array, whose antenna elements detect the correlated replicas of the data spectrum. The array adaptively combines them to produce the signal estimate. The concept is illustrated in Figure 2.9, with only the main lobes of the data spectrum replicas shown in the spread signal's spectrum.

It is even more useful to view the problem of DSSS-CDMA single-user detection in the time domain and then note its analogy with beamforming. The analogy applies both to the N-tap CHRT-LAR, as noted by Agee in [8], and the CW-FS-LAR. Both receivers use an adaptive linear filter to process the received signal. The mathematical model for the transversal filter is equivalent to the model for a narrowband linear equi-spaced adaptive antenna array, provided that the number of filter taps equals the number of antenna elements [24].

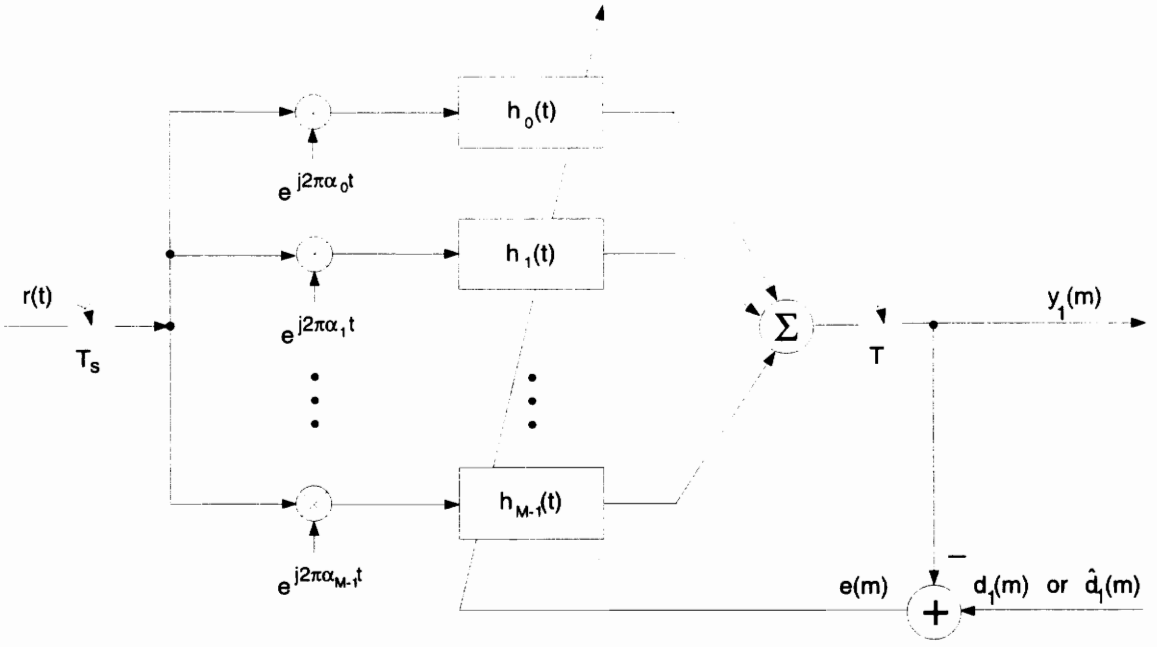

Figure 2.8: Fourier series representation time-dependent adaptive filter (FSR TDAF)

In case of DSSS-CDMA single-user detection the received signal is sampled in time, while in case of beamforming, it is sampled in space. The temporal or spatial samples of the received signal form a vector $\mathbf{r}$ which can be split into a desired signal term $\mathbf{r}_1$, an interference term $\mathbf{r}_i$, and a background noise term $\mathbf{n}$, i.e.,

$$\mathbf{r} = \begin{bmatrix} r_0 & r_1 & \cdots & r_{L-1} \end{bmatrix}^T = \mathbf{r}_1 + \mathbf{r}_i + \mathbf{n}, \tag{2.20}$$

where L is the number of filter taps or the number of antenna elements.

In case of code-on-pulse modulation, the desired DSSS signal vector can be written as

$$\mathbf{r}_1 = d_1 \cdot \mathbf{s}_1, \tag{2.21}$$

where d_1 is the data symbol being detected, and $\mathbf{s}_1$ is formed by the desired user's spreading waveform samples. In case of beamforming, $\mathbf{r}_1$ has the same form as given in (2.21), where d_1 contains the amplitude and time dependence of the desired signal, and s_1 is the steering vector corresponding to the desired signal's direction of arrival [25]. The steering vector contains the interelement phase shifts and element patterns.

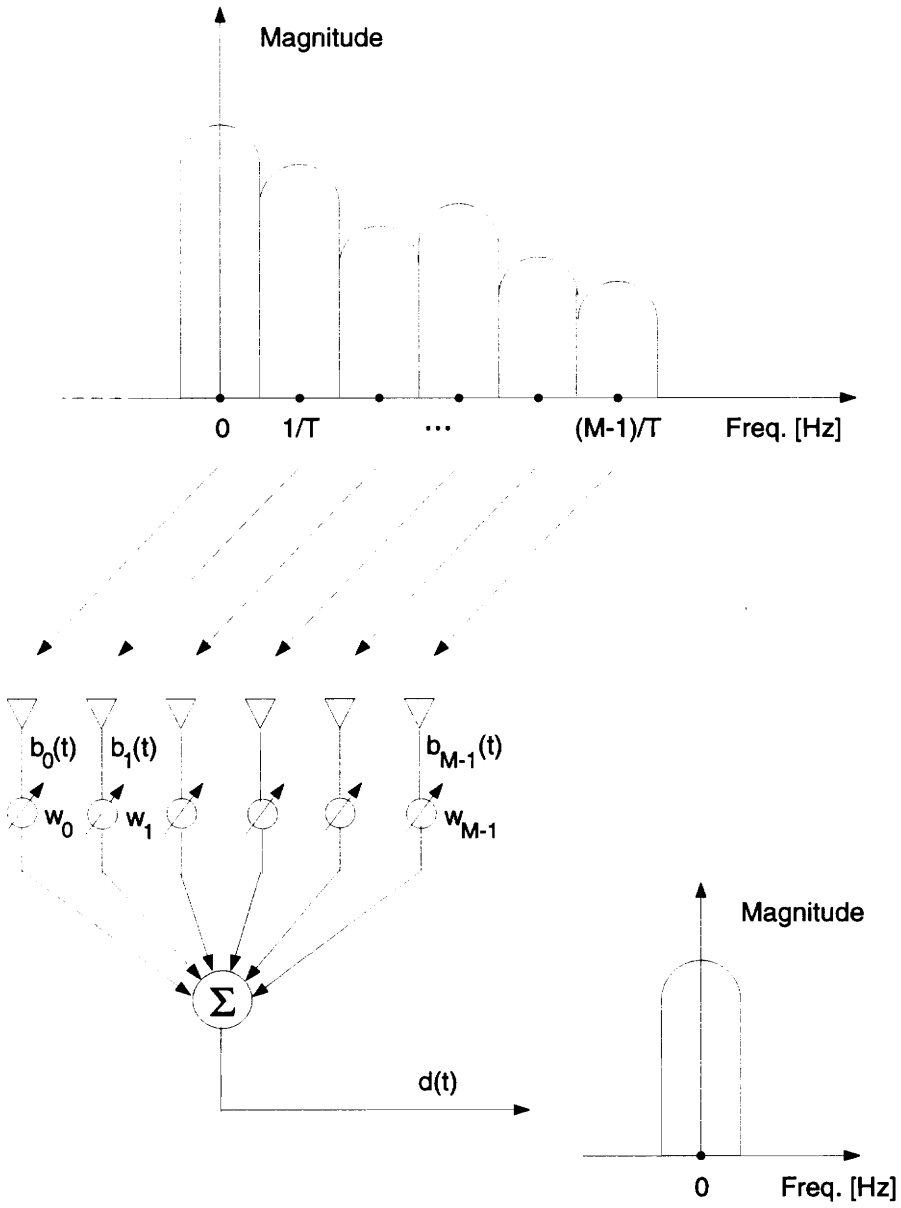

Figure 2.9: The analogy with beamforming in frequency domain

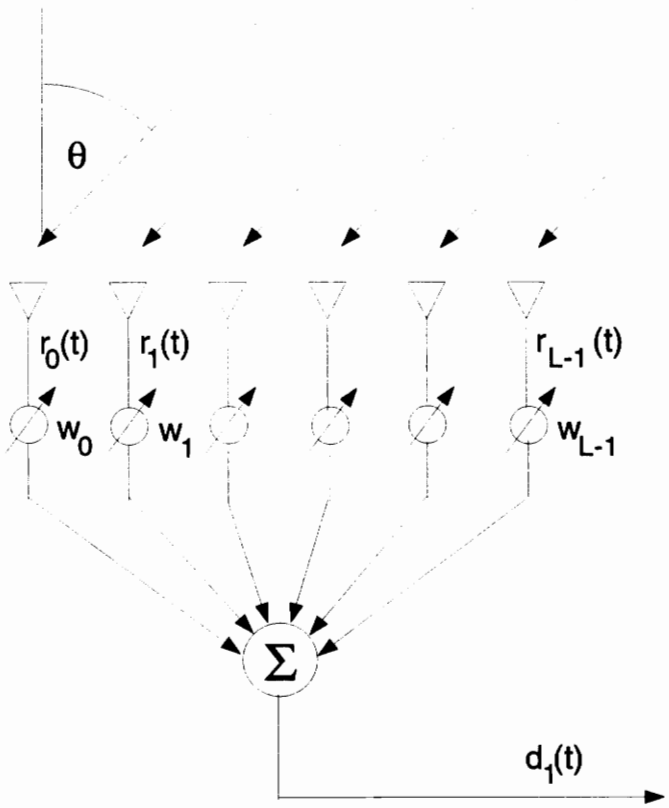

Figure 2.10: Narrowband linear equi-spaced adaptive antenna array

In case of L isotropic elements (Figure 2.10), the steering vector is given by

$$\mathbf{s}_1 = \begin{bmatrix} 1 & e^{-j\phi_1} & \cdots & e^{-j\phi_{L-1}} \end{bmatrix}^T, \tag{2.22}$$

where ϕ_l is the interelement phase shift between the lth and the 0th element,

$$\phi_l = \frac{2\pi L_l}{\lambda} \sin\theta, \tag{2.23}$$

L_l is the interelement spacing between the lth and the 0th element, $l = 1, 2, \ldots, L-1$, θ is the direction of arrival (DOA), and λ is the wavelength corresponding to the signal frequency.

It is seen that the two linear adaptive receivers for DSSS-CDMA single-user detection work similarly, at least mathematically speaking, to an adaptive antenna array

which seeks to form a beam pointed towards the signal of interest (SOI), thus detecting it and rejecting the signals not of interest (SNOI). Formulation of the symbol estimating DSSS-CDMA single-user receiver is identical to that of the adaptive antenna array. This analogy is of great importance, because it allows us to apply the beamforming concepts, ideas and techniques to the problem of DSSS-CDMA single-user detection. It proves most helpful with the search for adaptation algorithms appropriate for single-user detection, as seen in the next chapter.

Chapter 3

Adaptation Algorithms

The choice of the adaptation algorithm can greatly influence the performance of a single-user detector. It is preferred that the algorithm has low computational requirements, a fast convergence rate and that it is blind. The minimization of computational requirements is particularly important when the receiver is used for the mobile or portable unit, due to the weight, size and, therefore, complexity constraints. In the mobile communications environment, a fast convergence rate is important so that the algorithm is able to track the time-varying system parameters such as the quickly varying channel characteristics and the changing number of users. Blind adaptation algorithms that can converge even if the receiver starts with a "closed eye" are preferred to the trained ones. Such algorithms don't require a training sequence and the transmission needn't be interrupted for retraining when there is a sudden and large change in the system.

Our study of different adaptation algorithms and their simulation comparison are performed using the complex-weight fractionally-spaced linear adaptive receiver (CW-FS-LAR) described in Section 2.3.1. This particular receiver is chosen because it promises superior performance over the chip-rate receivers, and because of its mathematical simplicity. A performance comparison of different single-user detectors described in Chapter 2, adapted by a single trained adaptation algorithm, is found in [26]. All of the algorithms discussed in the coming sections can be used to adapt any of the receivers discussed in Chapter 2. The adaptation algorithms discussed in this section are divided into two groups, trained and blind algorithms.

3.1 Trained Adaptation Algorithms

Trained adaptation algorithms used for the adaptive single-user detectors discussed in Chapter 2 are the *least-mean-square (LMS)* algorithm, the *normalized LMS (NLMS)* algorithm, and the *recursive least-squares (RLS)* algorithm. Since it serves as a basis for deriving many other adaptation algorithms, including some of the blind algorithms presented, the LMS algorithm and its derivation will be presented in greater detail.

3.1.1 Least-Mean-Square (LMS) Adaptation Algorithm

An adaptation algorithm is designed to minimize a cost function chosen in such a way that, after convergence, the filter output is as close as possible to the desired signal. In the case of the CW-FS-LAR (Figure 2.5) these two signals are the signal estimate $y_1(m)$ and the data symbol $d_1(m)$.

The LMS algorithm minimizes the mean-squared error (MSE),

$$MSE = \mathrm{E}[|e(m)|^2], \tag{3.1}$$

where the error signal is given by

$$e(m) = d_1(m) - y_1(m), \qquad \text{or} \qquad e(m) = \hat{d}_1(m) - y_1(m), \tag{3.2}$$

depending on whether the algorithm is in the training or the decision-directed mode. The true data symbol and the hard decision estimate are denoted as $d_1(m)$ and $\hat{d}_1(m)$, respectively.

In the case of the CW-FS-LAR the filtering operation is modeled by

$$y_1(m) = \mathbf{w}^T \mathbf{r}(m), \tag{3.3}$$

where $\mathbf{w}$ is the filter weight vector of length L, $L \geq Np$,

$$\mathbf{w} = \begin{bmatrix} w_0 & w_1 & \cdots & w_{L-1} \end{bmatrix}^T, \tag{3.4}$$

and $\mathbf{r}(m)$ is the fractionally-spaced received signal vector at the mth symbol interval,

$$\mathbf{r}(m) = \begin{bmatrix} r_0(m) & r_1(m) & \cdots & r_{L-1}(m) \end{bmatrix}^T. \tag{3.5}$$

The received signal is sampled p times per chip, N is the processing gain, and the filter corresponds to at least one data symbol in length.

It can be shown that the optimum filter weights that yield the minimum MSE (MMSE) are found as the solution to the Wiener-Hopf equations [25], [27]–[29], given by

$$\mathbf{w}_{MMSE} = \mathbf{R}^{-1}\mathbf{p}, \tag{3.6}$$

where $\mathbf{R}$ is the correlation matrix of the input signal vector,

$$\mathbf{R} = \mathrm{E}[\mathbf{r}^*(m)\mathbf{r}^T(m)], \tag{3.7}$$

and $\mathbf{p}$ is the cross-correlation between the input vector and the desired output,

$$\mathbf{p} = \mathrm{E}[\mathbf{r}^*(m)d_1(m)]. \tag{3.8}$$

The Wiener-Hopf equations are derived by taking the gradient of the MSE cost function with respect to the weight vector and setting it equal to the zero vector [29],

$$\begin{aligned} \nabla_{\mathbf{w}}(MSE) &= \nabla_{\mathbf{w}}(\mathrm{E}[|d_1(m) - \mathbf{w}^T\mathbf{r}(m)|^2]) \\ &= \nabla_{\mathbf{w}}(\mathrm{E}[|d_1(m)|^2] - \mathbf{w}^H\mathbf{p} - \mathbf{p}^H\mathbf{w} + \mathbf{w}^H\mathbf{R}\mathbf{w}) \\ &= -2\mathbf{p} + 2\mathbf{R}\mathbf{w} = \mathbf{0}, \end{aligned} \tag{3.9}$$

where $[\cdot]^H$ denotes the conjugate transpose (Hermitian) operation.

It is seen that, for the optimum weight vector to be found, the second order statistics of the received signal are required. They are not available, however, one reason being that the other users' spreading codes are unknown. An adaptive algorithm is needed, designed so that the filter response converges to the statistically optimal solution given by (3.6).

The LMS adaptation algorithm is derived as a gradient search method and, moreover, a method of steepest descent [27]–[29]. It uses estimates for the gradient of the MSE cost function to search for the function's minimum. The weight vector is changed at each iteration cycle, in the direction of the negative gradient of the MSE with respect to the weight vector. The method of steepest descent that follows the MMSE criterion is given by

$$\begin{aligned} \mathbf{w}(m+1) &= \mathbf{w}(m) - \frac{\mu}{2}\nabla_{\mathbf{w}}(MSE) \\ &= \mathbf{w}(m) + \mu(\mathbf{p} - \mathbf{R}\mathbf{w}(m)), \end{aligned} \tag{3.10}$$

where μ is a step size that determines the algorithm's convergence rate and misadjustment [28]. The weight vector is updated every symbol interval.

The LMS algorithm is an approximate implementation of the method of steepest descent that uses instantaneous estimates for the correlation matrix $\mathbf{R}$ and the cross-correlation vector $\mathbf{p}$, given by

$$\hat{\mathbf{R}} = \mathbf{r}^*(m)\mathbf{r}^T(m), \tag{3.11}$$

and

$$\hat{\mathbf{p}} = \mathbf{r}^*(m)d_1(m). \tag{3.12}$$

The weight update equation is derived as

$$\begin{aligned} \mathbf{w}(m+1) &= \mathbf{w}(m) + \mu(\hat{\mathbf{p}} - \hat{\mathbf{R}}\mathbf{w}(m)) \\ &= \mathbf{w}(m) + \mu\mathbf{r}^*(m)d_1(m) - \mu\mathbf{r}^*(m)\mathbf{r}^T(m)\mathbf{w}(m) \\ &= \mathbf{w}(m) + \mu\mathbf{r}^*(m)d_1(m) - \mu\mathbf{r}^*(m)y_1(m). \end{aligned} \tag{3.13}$$

For the decision-directed mode, Equation (3.13) becomes

$$\mathbf{w}(m+1) = \mathbf{w}(m) + \mu\mathbf{r}^*(m)\hat{d}_1(m) - \mu\mathbf{r}^*(m)y_1(m). \tag{3.14}$$

The algorithm is then given by

$$\mathbf{w}(m+1) = \mathbf{w}(m) + \mu\mathbf{r}^*(m)e(m), \tag{3.15}$$

where the error signal $e(m)$ is defined by (3.2) for the two adaptation modes. The weight vector is initialized by

$$\mathbf{w}(0) = \mathbf{s}_1, \tag{3.16}$$

where $\mathbf{s}_1$ is the spreading code vector formed by sampling the desired user's spreading waveform, its length corresponding to the length of the filter.

The LMS adaptation algorithm is very simple and easy to implement, and it serves as a basis for the derivation of a number of other algorithms. One disadvantage of the LMS algorithm is its relatively slow convergence rate. Other faster converging trained algorithms, such as the NLMS and the RLS, are often used instead.

3.1.2 Normalized Least-Mean-Square (NLMS) Adaptation Algorithm

The NLMS adaptation algorithm is a modification of the LMS algorithm, with the step size μ chosen to provide faster convergence with a relatively small increase in the algorithm's complexity.

It can be shown that, for the LMS algorithm to be stable, the step size must be chosen to satisfy

$$0 < \mu < \frac{2}{\lambda_{max}}, \tag{3.17}$$

where λ_{max} is the largest eigenvalue of the correlation matrix $\mathbf{R}$ [27]–[30]. As the step size μ increases, the algorithm convergence becomes faster, but the misadjustment becomes larger. The misadjustment is a measure of how much the MSE that the algorithm achieves once it converges differs from the MMSE. The MMSE can never be achieved, because signal statistics estimates are used, rather than their true values. When the step size has a value which is outside the interval given in (3.17), the algorithm becomes unstable and diverges.

The NLMS algorithm uses a step size that is not a constant, but a function of the instantaneous estimate for the average power of the input signal (i.e., the instantaneous input power), to achieve a faster convergence rate than the LMS algorithm, while avoiding instability. The justification for this choice of the step size is found in the fact that

$$\lambda_{max} \leq \mathrm{E}[\mathbf{r}^T(m)\mathbf{r}^*(m)], \tag{3.18}$$

i.e., the maximum eigenvalue is limited by the input signal's average power [30].

The derivation of the NLMS algorithm is found in [30], and its weight update equation is given by

$$\mathbf{w}(m+1) = \mathbf{w}(m) + \frac{\alpha}{\gamma + \mathbf{r}^T(m)\mathbf{r}^*(m)}\mathbf{r}^*(m)e(m). \tag{3.19}$$

The step size is given by

$$\mu(m) = \frac{\alpha}{\gamma + \mathbf{r}^T(m)\mathbf{r}^*(m)}, \tag{3.20}$$

where α is a constant which determines the amount of misadjustment and is chosen so that $0 < \alpha < 2$, and γ is a small positive constant included to ensure that the step size is not excessively large when the instantaneous power is temporarily very small.

While the complexity of the LMS algorithm is of the order of L, where L is the dimension of the input signal vector, the complexity of the NLMS algorithm is somewhat larger. The number of multiplications is $2L$ instead of L, and the storage requirements are increased as well. Usually the increased computational requirements are justified by the considerably improved convergence rate.

3.1.3 Recursive Least-Squares (RLS) Adaptation Algorithm

The RLS algorithm is designed to minimize the exponentially weighted least-squares (LS) cost function, given by

$$LS(j) = \sum_{i=1}^{j} \rho^{j-i} |e(i)|^2, \tag{3.21}$$

where j is the duration of the observation interval, and ρ is the "exponential" weighting or forgetting factor, used to ensure that the data input in the distant past are "forgotten", so that the algorithm can follow the changes in the system and operate in a nonstationary environment.

Unlike the LMS and the NLMS algorithms, the RLS algorithm is not a gradient search method. Instead of using the gradient of the cost function to gradually converge to the function's minimum, it attempts to provide an exact solution to the minimization problem at every iteration. The algorithm uses the estimate for the weight vector computed at time $m-1$ as the *a priori solution* at time m. Based on the a priori solution and the data input at time m, the weight vector for time m, i.e., the *a posteriori solution*, is formed.

The algorithm is given by

$$\begin{aligned}
y_1^a(m) &= \mathbf{w}^T(m-1)\mathbf{r}(m), && (3.22)\\
e(m) &= d_1(m) - y_1^a(m), \quad \text{or} \quad e(m) = \hat{d}_1(m) - y_1^a(m), && (3.23)\\
\mathbf{z}(m) &= \mathbf{r}^H(m)\mathbf{R}^{-1}(m-1), && (3.24)\\
q &= \mathbf{z}(m)\mathbf{r}(m), && (3.25)\\
v &= \frac{1}{\rho + q}, && (3.26)\\
\hat{\mathbf{z}}(m) &= v\mathbf{R}^{-1}(m-1)\mathbf{r}(m), && (3.27)\\
\mathbf{w}(m) &= \mathbf{w}(m-1) + e(m)\hat{\mathbf{z}}^*(m), && (3.28)\\
\mathbf{R}^{-1}(m) &= \frac{1}{\rho}[\mathbf{R}^{-1}(m-1) - \hat{\mathbf{z}}(m)\mathbf{z}(m)], && (3.29)\\
y_1^p(m) &= \mathbf{w}^T(m)\mathbf{r}(m), && (3.30)
\end{aligned}$$

where $y_1^a(m)$ and $y_1^p(m)$ are the a priori and the a posteriori filter outputs at the mth symbol interval, respectively; $\mathbf{z}(m)$ is the gain vector; q is the normalized error power constant; v is the gain constant; $\hat{\mathbf{z}}(m)$ is the normalized gain vector; $e(m)$ is

the error signal; and $\mathbf{R}^{-1}(m)$ is the inverse of the input signal correlation matrix. The algorithm is initialized by

$$\mathbf{w}(0) = \mathbf{s}_1, \tag{3.31}$$

and

$$\mathbf{R}^{-1}(0) = \eta \cdot \mathbf{I}, \tag{3.32}$$

where η is a large positive constant, and $\mathbf{I}$ is the identity matrix of dimensions $L \times L$.

The RLS algorithm achieves a faster convergence and a smaller misadjustment than the LMS algorithm, at the cost of a large increase in computational complexity and storage requirements. While the computational requirements for the LMS and NLMS algorithms are of the order of L, for the RLS algorithm it is of the order of L^2.

3.2 New Blind Adaptation Algorithms for DSSS-CDMA Single-User Detection

Algorithms that are commonly proposed for adapting the single-user detection receiver structures are the trained adaptation algorithms discussed in the previous section. All of these algorithms require an initial adaptation involving the use of a training sequence. This means whenever a sudden and large change occurs in the system (i.e., a change in the number of users and the amount of MAI, or a change in the channel), data transmission is interrupted and cannot be resumed until the receiver weights are retrained using the training sequence.

To avoid the need for a training sequence blind algorithms are preferred, one option being to use decision-directed LMS, NLMS, or RLS adaptation. In this approach only decision-directed adaptation is used, i.e., there is no initial training phase utilizing a training sequence. Unfortunately, decision-directed adaptation suffers from "catastrophic failure" [15]. When there is enough interference so that the algorithm starts from a "closed eye", the hard decision error rate can be considerably high. The incorrect hard decisions are fed back and used by the algorithm as if they were correct. This can lead to algorithm's divergence, in which case the receiver output becomes independent of the transmitted data symbols (i.e., the algorithm fails catastrophically). This is why other blind algorithms are sought, ones that can satisfy the

requirements for the wireless and mobile communications environment, namely

1. convergence rates sufficiently fast to enable successful tracking of the quickly varying channel characteristics,
2. convergence even when starting from a "closed eye", and
3. minimal computational requirements.

Three blind adaptation algorithms novel in the area of DSSS-CDMA single-user detection are investigated, namely the *Griffiths' algorithm*, the *constant modulus algorithm (CMA)*, and the *linearly constrained constant modulus algorithm (LCCMA)*. These algorithms are commonly used to adapt antenna arrays for beamforming, but they can also be applied to DSSS-CDMA single-user detection, based on the analogy presented in Section 2.4.

3.2.1 Griffiths' Algorithm

The Griffiths' algorithm is first found as the adaptation algorithm for the Applebaum's antenna array. The array is based on the concept of maximizing the signal-to-interference-and-noise ratio (SINR) [25]. The SINR cost function is given by

$$SINR = \frac{P_1}{P_i + P_n}, \tag{3.33}$$

where P_1 is the desired signal power at the filter output,

$$P_1 = \frac{1}{2}\mathrm{E}[|\mathbf{w}^T\mathbf{r}_1(m)|^2], \tag{3.34}$$

P_i is the interference power at the filter output,

$$P_i = \frac{1}{2}\mathrm{E}[|\mathbf{w}^T\mathbf{r}_i(m)|^2], \tag{3.35}$$

and P_n is the background noise power at the filter output,

$$P_n = \frac{1}{2}\mathrm{E}[|\mathbf{w}^T\mathbf{n}(m)|^2]. \tag{3.36}$$

The received signal vector at the mth symbol interval $\mathbf{r}(m)$ is split into the desired signal term $\mathbf{r}_1(m)$, the interference term $\mathbf{r}_i(m)$, and the background noise term $\mathbf{n}(m)$, i.e.,

$$\mathbf{r}(m) = \mathbf{r}_1(m) + \mathbf{r}_i(m) + \mathbf{n}(m). \tag{3.37}$$

It is shown in [25], [31] that the SINR cost function can be written as

$$SINR = \mathrm{E}[|d_1(m)|^2]\frac{|\mathbf{w}^T\mathbf{s}_1|^2}{\mathbf{w}^H\mathbf{R}_{i,n}\mathbf{w}}, \tag{3.38}$$

where $d_1(m)$ is a scalar that contains the amplitude and time dependence of the desired signal at the mth symbol interval, $\mathbf{s}_1$ is the desired signal's steering vector, and $\mathbf{R}_{i,n}$ is the correlation matrix of the input interference and background noise,

$$\begin{aligned}\mathbf{R}_{i,n} &= \mathrm{E}[(\mathbf{r}_i(m)+\mathbf{n}(m))^*(\mathbf{r}_i(m)+\mathbf{n}(m))^T] \\ &= \mathrm{E}[\mathbf{r}_i(m)^*\mathbf{r}_i(m)^T] + \mathrm{E}[\mathbf{n}(m)^*\mathbf{n}(m)^T].\end{aligned} \tag{3.39}$$

The derivation for the optimum antenna array weights that yield the maximum SINR (MSINR) is found in [25], [31], and the weights are given by

$$\mathbf{w}_{MSINR} = \nu_1\mathbf{R}_{i,n}^{-1}\mathbf{s}_1^*, \tag{3.40}$$

where ν_1 is an arbitrary scalar constant. Applebaum proposed an adaptation algorithm [25], which converges to the weights given by

$$\mathbf{w} = \nu\mathbf{R}^{-1}\mathbf{s}_1^*, \tag{3.41}$$

where ν is an arbitrary scalar constant, and $\mathbf{R}$ is the correlation matrix of the input signal,

$$\mathbf{R} = \mathrm{E}[\mathbf{r}(m)^*\mathbf{r}(m)^T]. \tag{3.42}$$

It is seen that (3.40) and (3.41) are different, but it can be shown that the terms $\mathbf{R}_{i,n}^{-1}\mathbf{s}_1^*$ and $\mathbf{R}^{-1}\mathbf{s}_1^*$ produce weight vectors which are integrally related and both optimum in the MSINR sense [25]. The algorithm proposed by Applebaum is given by

$$\mathbf{w}(m+1) = \mathbf{w}(m) + \mu\nu\mathbf{s}_1^* - \mu\mathbf{r}^*(m)y_1(m), \tag{3.43}$$

where μ is the constant step size, and $y_1(m)$ is the array output.

Following the analogy described in Section 2.4, the adaptation algorithm used for the Applebaum's array can be used to adapt the CW-FS-LAR. In this case $\mathbf{s}_1$ is the spreading code vector formed by the desired user's spreading waveform samples corresponding to the portion of the input signal contained in the filter, $\mathbf{r}(m)$ is the received signal vector at the mth symbol interval, and $y_1(m)$ is the filter output.

The starting point for Griffiths' derivation, which led to the same algorithm as the one used for the Applebaum's array, is the MMSE criterion [30]. Griffiths derived the algorithm as an approximate implementation of the method of steepest descent that follows the MMSE criterion, assuming that the cross-correlation vector $\mathbf{p}$ (defined by Equation (3.8)) is known.

The method of steepest descent was introduced in Section 3.1.1, and is given by

$$\mathbf{w}(m+1) = \mathbf{w}(m) + \mu(\mathbf{p} - \mathbf{R}\mathbf{w}(m)). \tag{3.44}$$

Just like the LMS algorithm, the Griffiths' algorithm uses the instantaneous estimate for the correlation matrix $\mathbf{R}$,

$$\hat{\mathbf{R}} = \mathbf{r}^*(m)\mathbf{r}^T(m), \tag{3.45}$$

but it uses the true value of the cross-correlation vector $\mathbf{p}$. The weight update equation is derived as

$$\begin{aligned}
\mathbf{w}(m+1) &= \mathbf{w}(m) + \mu(\mathbf{p} - \hat{\mathbf{R}}\mathbf{w}(m)) \\
&= \mathbf{w}(m) + \mu\mathbf{p} - \mu\mathbf{r}^*(m)\mathbf{r}^T(m)\mathbf{w}(m) \\
&= \mathbf{w}(m) + \mu\mathbf{p} - \mu\mathbf{r}^*(m)\mathbf{w}^T(m)\mathbf{r}(m) \\
&= \mathbf{w}(m) + \mu\mathbf{p} - \mu\mathbf{r}^*(m)y_1(m).
\end{aligned} \tag{3.46}$$

In the case of beamforming, the cross-correlation vector $\mathbf{p}$ is equal to the conjugated steering vector for the desired user, and in the case of DSSS-CDMA single-user detection it is equal to the conjugated desired user's spreading code, which is given by

$$\begin{aligned}
\mathbf{p} &= \mathrm{E}[\mathbf{r}^*(m)d_1(m)] \\
&= \mathrm{E}[\mathbf{r}_1^*(m)d_1(m)] + \mathrm{E}[\mathbf{r}_i^*(m)d_1(m)] + \mathrm{E}[\mathbf{n}^*(m)d_1(m)] \\
&= \mathrm{E}[\mathbf{r}_1^*(m)d_1(m)] \\
&= \mathrm{E}[|d_1(m)|^2\mathbf{s}_1^*] \\
&= \mathbf{s}_1^*.
\end{aligned} \tag{3.47}$$

The derivation (3.47) is based on the fact that the detected data symbol $d_1(m)$ is uncorrelated with the interference, or the background noise.

The Griffiths' algorithm applied to DSSS-CDMA single-user detection is thus given by

$$\mathbf{w}(m+1) = \mathbf{w}(m) + \mu(\mathbf{s}_1^* - \mathbf{r}^*(m)y_1(m)) \tag{3.48}$$

$$\mathbf{w}(0) = \mathbf{s}_1. \tag{3.49}$$

It is interesting to note that the Griffiths algorithm is the algorithm proposed by Applebaum, for $\nu = 1$, and that the first converges to the MMSE weights and the second to the MSINR weights. It is seen that the MMSE weights are given by

$$\begin{aligned} \mathbf{w}_{MMSE} &= \mathbf{R}^{-1}\mathbf{p} \\ &= \mathbf{R}^{-1}\mathbf{s}_1^*, \end{aligned} \tag{3.50}$$

which correspond to the MSINR weights given by Equation (3.41).

Comparing the computational requirements of the Griffiths' algorithm with the LMS algorithm, the computational complexity and storage requirements for the Griffiths' algorithm are slightly greater, but are of the same order. The number of multiplications is the same, but the number of subtractions is increased because two vectors are subtracted, instead of two scalars, as in the case of the LMS. The desired user's spreading code needs to be stored on top of the step size. Unlike the LMS algorithm, however, the Griffiths' algorithm is blind and, instead of using a reference signal (i.e., a training sequence or the fed-back decision), it utilizes the desired user's spreading waveform.

3.2.2 Constant Modulus Algorithm (CMA)

The CMA and other algorithms derived from it minimize a cost function which exploits the constant envelope of the modulated signal. Instead of a training sequence, the algorithm uses the constant modulus property and adapts the filter in order to restore/maintain this property [32]. In Section 2.1 BPSK modulation was assumed for the considered DSSS-CDMA system. Since BPSK modulated signals are constant modulus, the CMA is considered a candidate for the adaptation algorithm for DSSS-CDMA single-user detection.

The constant modulus (CM) cost function is given by

$$CM = \frac{1}{4}\mathrm{E}[(|y_1(m)|^2 - \delta)^2], \tag{3.51}$$

where δ is the expected or estimated value for the desired user's received signal power. It is assumed that $\delta = 1$. Similar to the LMS algorithm, the CMA is an approximate implementation of a gradient search method, one that searches for the minimum of the CM cost function. As shown in [33], the method is derived by

$$\begin{aligned}
\mathbf{w}(m+1) &= \mathbf{w}(m) - \mu\nabla_{\mathbf{w}}(CM) && (3.52)\\
&= \mathbf{w}(m) - \frac{\mu}{4}\mathrm{E}[2(|y_1(m)|^2 - 1)\nabla_{\mathbf{w}}(y_1^*(m)y_1(m))]\\
&= \mathbf{w}(m) - \frac{\mu}{2}\mathrm{E}[(|y_1(m)|^2 - 1)\nabla_{\mathbf{w}}(\mathbf{w}^H\mathbf{r}^*(m)\mathbf{r}^T(m)\mathbf{w})]\\
&= \mathbf{w}(m) - \frac{\mu}{2}\mathrm{E}[(|y_1(m)|^2 - 1)\cdot 2\mathbf{r}^*(m)\mathbf{r}^T(m)\mathbf{w}]\\
&= \mathbf{w}(m) - \mu\mathrm{E}[(|y_1(m)|^2 - 1)\mathbf{r}^*(m)y_1(m)]. && (3.53)
\end{aligned}$$

The CMA, which uses the instanteneous estimate for the cost function's gradient, is given by

$$\mathbf{w}(m+1) = \mathbf{w}(m) - \mu(|y_1(m)|^2 - 1)\mathbf{r}^*(m)y_1(m), \tag{3.54}$$

and is initialized by

$$\mathbf{w}(0) = \mathbf{s}_1. \tag{3.55}$$

The CMA is a blind adaptation algorithm whose weight update equation (3.54) is similar to that of the LMS algorithm (3.15). In fact, the two updates will be exactly the same, if we define the CMA "error signal" by

$$e_{CMA}(m) = (|y_1(m)|^2 - 1)y_1(m), \tag{3.56}$$

and use this error in Equation (3.15). Therefore, the complexity of the CMA is slightly larger than that of the LMS algorithm, due to the larger computational requirements for the error signal.

One disadvantage of the CMA is that it may capture a constant modulus signal other than the desired one [36]. The problem stems from the fact that the CM cost function doesn't have a unique minimum, and that it will be minimized for any constant modulus filter output. Since all the MAI signals in a CDMA system have a constant modulus, a single-user detector adapted using the CMA might fail in detecting the desired user's signal and capture an interferer instead. It may be possible to control the capture problem by appropriately choosing the initial value for the filter weights. By initializing the adaptive filter with the spreading code of the desired user, the CMA is pointed in the right direction. Another option is to

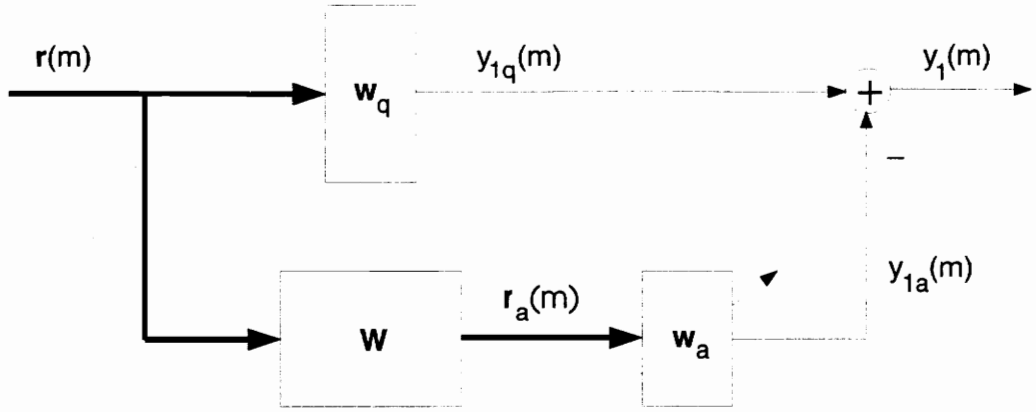

Figure 3.1: Generalized sidelobe canceller (GSC)

use the linearly constrained constant modulus algorithm (LCCMA), discussed in the next section.

3.2.3 Linearly Constrained Constant Modulus Algorithm (LCCMA)

The LCCMA was first proposed in [36], as a method of controlling the behavior of the CMA, which sometimes nulls the desired signal and passes an undesired one. The constant modulus adaptation is performed with the weight vector under a set of linear constraints,

$$\mathbf{C}^H\mathbf{w} = \mathbf{f}, \tag{3.57}$$

where $\mathbf{C}$ is a constant matrix of dimensions $L \times L_{lc}$, $\mathbf{f}$ is a constant column vector of length L_{lc}, L_{lc} is the number of linear constraints, $L_{lc} < L$, and L is the length of the weight vector $\mathbf{w}$.

The constrained problem of minimizing the CM cost function can be converted to an unconstrained minimization problem by using a preprocessor known as the *generalized sidelobe canceller (GSC)* [36], shown in Figure 3.1. The preprocessor splits the weight vector into a constrained component and an unconstrained one, such that

$$\mathbf{w} = \mathbf{w}_q - \mathbf{W}\mathbf{w}_a, \tag{3.58}$$

where $\mathbf{w}_q$ is the constrained fixed portion of the weight vector, of length L, given by

$$\mathbf{w}_q = \mathbf{C}(\mathbf{C}^H\mathbf{C})^{-1}\mathbf{f}, \tag{3.59}$$

and $\mathbf{w}_a$ is the portion that is adapted, of length $L - L_{lc}$. The reduction matrix $\mathbf{W}$ is chosen so that its columns span the left nullspace of $\mathbf{C}$, i.e.,

$$\mathbf{C}^H\mathbf{W} = \mathbf{0}, \tag{3.60}$$

and its dimensions are $L \times (L - L_{lc})$. As shown in [36], $\mathbf{w}_q$ and $\mathbf{W}$ given by (3.59) and (3.60) satisfy the linear constraints in (3.57),

$$\begin{aligned} \mathbf{C}^H\mathbf{w} &= \mathbf{C}^H(\mathbf{w}_q - \mathbf{W}\mathbf{w}_a) \\ &= (\mathbf{C}^H\mathbf{C})(\mathbf{C}^H\mathbf{C})^{-1}\mathbf{f} - (\mathbf{C}^H\mathbf{W})\mathbf{w}_a \\ &= \mathbf{f}. \end{aligned} \tag{3.61}$$

It is also seen that (3.57) is satisfied for any choice of $\mathbf{w}_a$, which means that the adaptive portion of the weight vector is unconstrained. The CM cost function is then minimized using the instantaneous estimate for its gradient taken with respect to $\mathbf{w}_a$, and the $\mathbf{w}_a$ update equation is given by

$$\mathbf{w}_a(m+1) = \mathbf{w}_a(m) + \mu(|y_1(m)|^2 - 1)\mathbf{r}_a^*(m)y_1(m). \tag{3.62}$$

For DSSS-CDMA single-user detection a proper choice for the linear constraints would be to pass the desired user's signal with unity gain and to null the interfering signals. Matrix $\mathbf{C}$ would have the first column equal to the desired user's spreading code, and spreading codes of the $L_{lc} - 1$ strongest interferers would be chosen for the other columns. The free-coefficient vector would be $\mathbf{f} = \begin{bmatrix} 1 & 0 & \cdots & 0 \end{bmatrix}^T$. However, the basic assumption for single-user detection is that the interferers' spreading codes are unknown. Since the interferers' spreading codes are unknown, a single constraint is used, given by

$$\mathbf{s}_1^* \cdot \mathbf{w} = ||\mathbf{s}_1||^2 = 1. \tag{3.63}$$

It is assumed that the desired user's spreading waveform is normalized to have unit energy, and the dot product of two vectors $\mathbf{a}$ and $\mathbf{b}$ is denoted as $\mathbf{a} \cdot \mathbf{b}$. The constraint given by (3.63) is equivalent to the constraint

$$\mathbf{w} = \mathbf{s}_1 + \mathbf{w}_{adapt}, \qquad \text{where} \qquad \mathbf{s}_1 \cdot \mathbf{w}_{adapt} = 0, \tag{3.64}$$

which was used in [39] for linearly-constrained minimum output-energy adaptation. It is seen that the chosen constraint forces the weight vector to have a component responsible for the detection of the desired user's signal, and a component orthogonal to it, responsible for rejecting the interferers. This makes it impossible for the filter to capture an interferer instead of the desired signal.

The constraint (3.63) can be written in matrix form as

$$\mathbf{C}^H\mathbf{w} = \mathbf{f}, \tag{3.65}$$

where $\mathbf{C} = \mathbf{s}_1$, $\mathbf{f} = 1$ and $L_{lc} = 1$. The unconstrained portion of the weight vector based on (3.59) is

$$\begin{aligned} \mathbf{w}_q &= \mathbf{C}(\mathbf{C}^H\mathbf{C})^{-1}\mathbf{f} \\ &= \mathbf{s}_1(\mathbf{s}_1^H\mathbf{s}_1)^{-1} \\ &= \mathbf{s}_1, \end{aligned} \tag{3.66}$$

i.e., $\mathbf{w}_q$ is equal to the desired user's spreading code, which is consistent with (3.64). The reduction matrix $\mathbf{W}$ is chosen based on (3.60) such that

$$\mathbf{s}_1^H\mathbf{W} = \mathbf{0}, \tag{3.67}$$

and its dimensions are $L \times (L-1)$. In order to determine $\mathbf{W}$, first define matrix $\mathbf{A}$ which has dimensions $L \times L$,

$$\mathbf{A} = \begin{bmatrix} \mathbf{s}_1^H \\ \mathbf{0} \\ \vdots \\ \mathbf{0} \end{bmatrix}, \tag{3.68}$$

where the first row is $\mathbf{s}_1^H$, the conjugated desired user's spreading code, and the remaining $L-1$ rows are zero vectors. The $L-1$ eigenvectors of matrix $\mathbf{A}$, corresponding to the $L-1$ zero eigenvalues, are used for the columns of the reduction matrix $\mathbf{W}$, in order to satisfy (3.67). The reduction matrix $\mathbf{W}$ is thus given by

$$\mathbf{W} = \begin{bmatrix} \mathbf{e}_1 & \mathbf{e}_2 & \cdots & \mathbf{e}_{L-1} \end{bmatrix}, \tag{3.69}$$

where $\mathbf{e}_l$ is the lth eigenvector corresponding to the zero eigenvalue of matrix $\mathbf{A}$, such that

$$\mathbf{A} \cdot \mathbf{e}_l - 0 \cdot \mathbf{e}_l = \mathbf{0}, \tag{3.70}$$

for every l, $l = 1, 2, \ldots, L-1$.

The algorithm is then given by

$$\mathbf{w}_a(0) = \begin{bmatrix} 0 & 0 & \cdots & 0 \end{bmatrix}, \tag{3.71}$$

$$\mathbf{w}(m) = \mathbf{s}_1 - \mathbf{W}\mathbf{w}_a(m), \tag{3.72}$$

$$y_1(m) = \mathbf{w}^T\mathbf{r}(m), \tag{3.73}$$

$$\mathbf{r}_a(m) = \mathbf{W}\mathbf{r}(m), \tag{3.74}$$

$$\mathbf{w}_a(m+1) = \mathbf{w}_a(m) + \mu(|y_1(m)|^2 - 1)\mathbf{r}_a^*(m)y_1(m). \tag{3.75}$$

The complexity of the LCCMA is somewhat larger than the CMA and the Griffiths' algorithms. In each iteration cycle, the reduced-size input vector $\mathbf{r}_a$ needs to be calculated, as well as the weight vector $\mathbf{w}$, based on its updated adaptive portion $\mathbf{w}_a$. The values for the desired user's spreading code and the reduction matrix need to be stored as well.

Except for the increased computational and storage requirements, the LCCMA has another disadvantage, the need to estimate the desired user's received power δ (3.51). In this work it is assumed that δ is known and normalized to 1. In practice, however, this will not be necessarily true. As noted in [36], not knowing the exact value of δ will not present a crucial problem for the CMA. The weight vector is unconstrained and will be adapted to scale the received signal to fit the assumed value for δ. The CM property will still be restored. This will not be true for the LCCMA, which has a constrained weight vector and, therefore, a constrained gain. The LCCMA requires a good estimate for the signal power δ. An adaptive method for estimating δ,

$$\delta(m+1) = \delta(m) + \mu(|y_1(m)|^2 - \delta(m)), \tag{3.76}$$

is proposed in [36], [38].

3.3 Adaptation Algorithms' Computational and Storage Requirements Compared

We conclude the chapter on adaptation algorithms for DSSS-CDMA single-user detection by comparing their computational and storage requirements in more detail. The complexity of the blind algorithms and how it compares to the complexity of

Table 3.1: Comparison of Different Algorithms' Computational and Storage Requirements

Adaptation Algorithm	Number of Multiplications	Stored Parameters
LMS	$L+1$	μ
NLMS	$2L+1$	α, γ
RLS	$2L^2+3L$	ρ
Griffiths' algorithm	$L+1$	μ, $\mathbf{s}_1^*$
CMA	$L+3$	μ
LCCMA	$2L^2-L+2$	μ, $\mathbf{s}_1$, $\mathbf{W}$

the trained ones is of special interest. Table 3.1 shows the computational and storage requirements of the discussed trained and blind adaptation algorithms. The computational requirements are presented in terms of the number of multiplications per iteration, and the storage requirements in terms of the permanently stored quantities required for the adaptation.

It is seen that the RLS is the most complex algorithm. Not only that the largest number of multiplications is required in each iteration, but the adaptation also consists of the most number of updating steps, during which various quantities need to be stored on temporary basis (e.g., $\mathbf{R}^{-1}(m-1)$, $\mathbf{z}(m)$, and $\hat{\mathbf{z}}(m)$, defined in Section 3.1.3).

The storage requirements of the two blind algorithms are larger than in the case of LMS and NLMS. There is a trade-off between the requirement for storing certain known parameters of the desired signal in the case of blind adaptation and the requirement for a training sequence in the case of trained adaptation. It is very important to note that in terms of the number of multiplications the computational requirements of the Griffiths' algorithm are the same as those of the LMS. There is a slight increase in complexity for the Griffiths' algorithm, due to an increased number of subtractions, as discussed in Section 3.2.1. The complexity of the LCCMA is of the order of L^2, larger than that of the Griffiths' algorithm. Such computational requirements, as well as the larger storage requirements, and the need for a good estimate of the desired signal's power could make the choice of the LCCMA for DSSS-CDMA single-user detection unfavorable. The choice will depend, however, on how the performances of the two blind adaptation algorithms compare.

Chapter 4

Simulation Results

In this chapter the performance of the complex-weight fractionally-spaced linear adaptive receiver (CW-FS-LAR) adapted using the blind adaptation algorithms discussed in the previous section is investigated through Monte Carlo simulations. As indicated in Section 3.2 blind adaptation algorithm involves a small increase in complexity and computational requirements over the LMS algorithm. Through simulations performed on a Sun Microsystem SPARC workstation using MATLAB signal processing software and custom scripts the algorithms' convergence rates are investigated, as well as whether they suffer from catastrophic failure, as defined in Section 3.2. The blindly-adapted single-user detector's capability to detect the signal, reject the interference and provide near-far resistance is also explored. Its performance is compared to the conventional receiver and single-user detector adapted using a trained adaptation algorithm, NLMS. The simulations involve different scenarios in which single-user detection could be used.

The simulated CDMA signal is a sum of different users' DSSS BPSK-modulated signals, which are transmitted simultaneously over an AWGN channel. Code-on-pulse modulation is employed, with a processing gain of 15, and spreading is performed using randomly generated spreading codes. Different sets of codes with varying cross-correlation properties are used. The data rate is 128 kbps and the chip rate is 1.92 Mchips/sec.

The complex envelope of the bandpass background noise is a complex white Gaussian process, defined in Section 2.1 by

$$n(t) = n_r(t) + j \cdot n_i(t). \tag{4.1}$$

The two real baseband white Gaussian noise processes $n_r(t)$ and $n_i(t)$ have variances given by

$$\sigma_r^2 = \sigma_i^2 = \frac{1}{2} \cdot 10^{-SNR/10}, \tag{4.2}$$

where SNR is the pre-despread signal-to-noise ratio, chosen to be -6 dB or -9 dB. This corresponds to an E_b/N_0 of 5.76 dB and 2.76 dB, respectively. The desired user's signal power is normalized to be equal to 1, and the relationship between the SNR and the E_b/N_0 is given by

$$\begin{aligned} SNR &= \frac{E_b \cdot R}{N_0 \cdot B} \\ &= \frac{E_b}{N_0} \cdot \frac{1}{B/R} \\ &= \frac{E_b}{N_0} \cdot \frac{1}{N}, \end{aligned} \tag{4.3}$$

where E_b is the signal energy per data symbol; R is the data rate; N_0 is the power spectral density of the bandpass background noise; B is the bandwidth; and N is the processing gain.

The receiver is assumed to be perfectly synchronized with the desired user's signal, whose power is normalized, i.e., as assumed in Section 2.1, $P_{r1} = 1$, $\tau_1 = 0$, $\Delta\omega_1 = 0$, and $\theta_1 = 0$. The receiver samples the signal 3 times per chip, or 45 times per symbol period, i.e., the sampling rate and sampling period are 5.76 MHz and 17.3 μsec, respectively. The length of the adaptive filter is chosen to be 45, so that all 45 samples corresponding to a single spread data symbol are contained in the filter at the time when the receiver performs symbol detection. The step size, μ, which figures in the weight update equations for the three investigated blind adaptation algorithms (Section 3.2), is chosen through a trial-and-error procedure for every simulated scenario. Good convergence rate and misadjustment are sought, taking into account the trade-off between the two.

4.1 Zero-Forcing Capabilities of the CW-FS-LAR Adapted Using Blind Adaptation Algorithms: Performance Demonstration

To demonstrate that blind adaptation algorithms can be used for DSSS-CDMA single-user detection, the receiver's zero-forcing capability is investigated. In Section 3.2.3 it was argued that a proper choice for the LCCMA linear constraints would pass the desired user's signal with unity gain and null the interfering signals. The receiver would implement the zero-forcing solution, where the weight vector of the adaptive filter would be orthogonal to the interferers' spreading codes, and its dot product with the desired user's spreading code would be equal to 1. Again there is an analogy with beamforming, where unity gain is provided in the direction of the desired signal and nulls are forced in the direction of the interferers.

The fact that a single-user detector adapted according to the MMSE criterion, namely the N-tap CHRT-LAR, implements the zero-forcing solution when the power of the background noise tends to zero was discussed in [5]–[7], [40]. Since the model for the CW-FS-LAR is the same as for the N-tap CHRT-LAR, except that the fractionally-spaced filter weight vector is longer (Figure 2.2 and Figure 2.5), the same will be true for the CW-FS-LAR.

In both cases, in a system with K synchronous users and no background noise, the received signal vector at the mth symbol interval can be written as

$$\begin{aligned} \mathbf{r}(m) &= \sum_{k=1}^{K} \mathbf{r}_k(m) \\ &= \sum_{k=1}^{K} \sqrt{P_{rk}} d_k(m) \mathbf{s}_k, \end{aligned} \tag{4.4}$$

where $\mathbf{r}_k(m)$, P_{rk}, $d_k(m)$ and $\mathbf{s}_k$ are the kth user's received signal vector, received signal power, data symbol and spreading code, respectively. The filter output when the 1st user's signal is detected is given by

$$\begin{aligned} y_1(m) &= \mathbf{w}^T \mathbf{r}(m) \\ &= \sum_{k=1}^{K} \sqrt{P_{rk}} d_k(m) \mathbf{w}^T \mathbf{s}_k \\ &= \sum_{k=1}^{K} \sqrt{P_{rk}} d_k(m) \rho_k, \end{aligned} \tag{4.5}$$

where ρ_k is the measure of the cross-correlation between the weight vector and the kth user's spreading code. The MSE can then be written as

$$\begin{aligned} MSE &= \mathrm{E}[|d_1(m) - y_1(m)|^2] \\ &= \mathrm{E}[|d_1(m)(1-\rho_1) - \sum_{k=2}^{K} \sqrt{P_{rk}} d_k(m)\rho_k|^2]. \end{aligned} \tag{4.6}$$

Since different users' data signals are mutually independent, and assuming that the adaptation algorithm has already converged and the weight vector is approximately constant (i.e., $\mathbf{w} = \mathbf{w}_{MMSE}$), the MSE can further be written as

$$\begin{aligned} MSE &= \mathrm{E}[|d_1(m)(1-\rho_1)|^2] - \sum_{k=2}^{K} \mathrm{E}[|\sqrt{P_{rk}} d_k(m)\rho_k|^2] \\ &= |1-\rho_1|^2 - \sum_{k=2}^{K} |\sqrt{P_{rk}}\rho_k|^2. \end{aligned} \tag{4.7}$$

It is seen that as $MSE \to 0$, $\rho_1 \to 1$ and $\rho_k \to 0$ for $k = 2, 3, \ldots, K$, i.e., the receiver implements the zero-forcing solution.

When the power of the background noise is not zero, the receiver provides an approximate zero-forcing solution. The *decorrelating detector* of [41] is a multiuser detector which zeroes out the multiple-access interferers, but enhances the noise. The N-tap CHRT-LAR balances the effects of noise and interference, seeking to minimize the MSE [5]–[7].

No matter which adaptation algorithm is used and which cost function is minimized, a single-user detector's ability to reject interference will depend on how well it approximates the zero-forcing solution. Figure 4.1 shows the cross-correlation of the CW-FS-LAR weight vector for different users' spreading codes. These results are based on the adaptation algorithm having converged, specifically after 5000 transmitted data symbols. The three blind adaptation algorithms are investigated, namely the Griffiths' algorithm, the CMA and the LCCMA. For comparison purposes the cross-correlation values for the conventional detector (a non-adaptive receiver) are also presented.

The simulated system consists of 10 synchronous equal-power users and uses randomly generated spreading codes. The SNR is -6 dB. The magnitudes of the dot products of the weight vector and the spreading codes, $|\mathbf{w}^T\mathbf{s}_k|$, are shown ($k = 1, 2, \ldots, 10$). In the case of the conventional detector (i.e., the CW-FS-LAR with

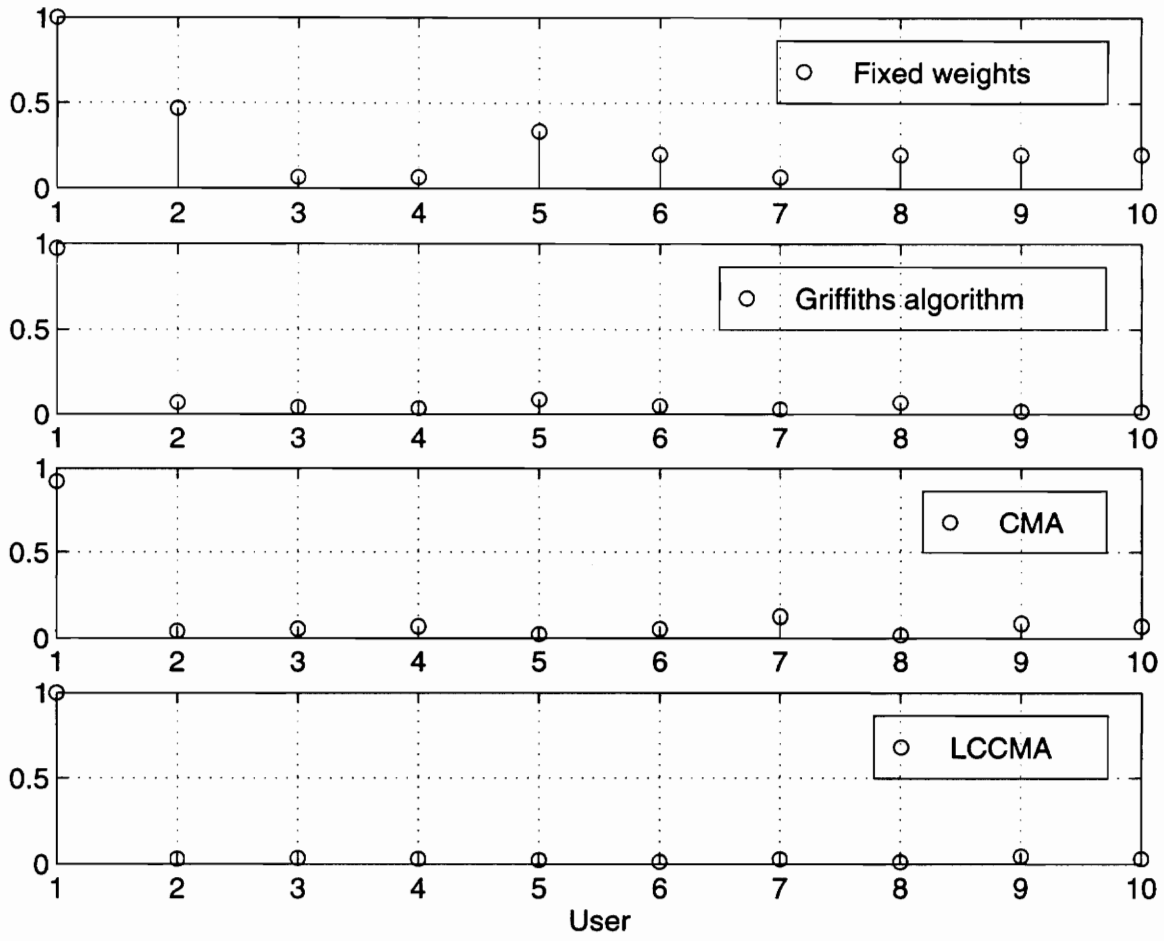

Figure 4.1: Cross-correlation $|\mathbf{w}^T\mathbf{s}_k|$ between the weight vector and the users' spreading codes, $k = 1, 2, \ldots, 10$, after 5000 transmitted data symbols

a fixed weight vector equal to the desired user's spreading code), they are equal to the cross-correlations between the desired user's spreading code and the interferers' spreading codes. At the same time the quantity $|\mathbf{w}^T\mathbf{s}_k|^2$ indicates the percentage of the kth user's received signal energy that is passed to the receiver output, thus showing how much of the desired signal is passed and how much of the interference is rejected.

Figure 4.1 shows that the CW-FS-LAR implements an approximate zero-forcing solution in all three blind adaptation cases. This is true even though the cross-correlation properties of the used set of spreading codes are poor. Users 2 ad 5 are the two strongest interferers, with a cross-correlation with the desired user's spreading

code of 0.47 and 0.33, respectively. The adaptive receiver passes the desired user's signal with a gain approximately equal to 1 (minimum 0.92 in the case of CMA), or exactly equal to 1 (in the case of LCCMA), and nulls all the interferers, or passes them with a very low gain (maximum 0.12 in the case of CMA). It is seen that the CMA performs worst and LCCMA best, but in all three blind adaptation cases there is a great improvement in interference rejection capability over conventional detection.

The potential problem of capturing an interferer's signal while using CMA was discussed in Section 3.2.2. Figure 4.2 illustrates this problem. The cross-correlation between the weight vector and users' spreading codes is shown after 2 million transmitted data symbols, based on the same system simulation parameters specified above. Comparing Figures 4.1 and 4.2 it is seen that the CMA, after the initial convergence to an approximate zero-forcing solution, diverges from it and finds a constant modulus (CM) solution that passes the desired signal with a gain of only 0.2, but captures an interferer, user 4, with a gain of 0.9. The receiver is actually detecting another user's signal. The explanation for such behavior is found in the fact that the algorithm is initialized with the desired user's spreading code, and is thus pointed towards a CM solution that rejects the interference. With time the algorithm gradually "forgets" this information and finds other CM solutions, out of the infinite set of possible ones, that needn't provide a low MSE and interference rejection capability.

It is concluded that just the knowledge of the desired signal's CM property is not enough for successfully detecting the desired signal. The knowledge of a characteristic of the desired signal that distinguishes it from other users' signals, such as its spreading code, must also be provided and continuously present. This is achieved with the LCCMA, for which the desired user's spreading code is made part of the processing operation, and whose performance seen in Figure 4.2 is as good as that seen in Figure 4.1. Similarly, the Griffiths' algorithm performs well and can be viewed as the LMS algorithm made blind by making use of the knowledge of the desired user's spreading code, which is made part of the weight update.

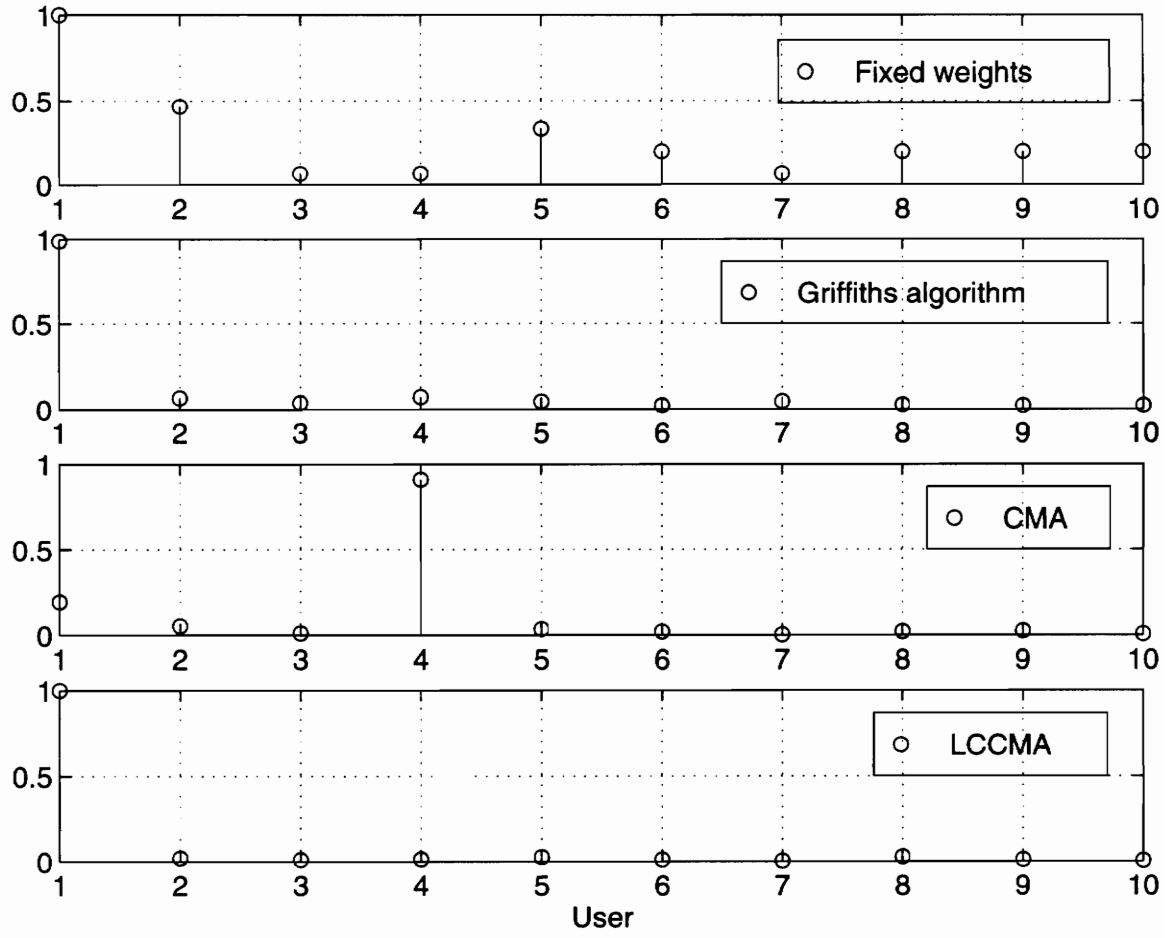

Figure 4.2: Cross-correlation $|\mathbf{w}^T\mathbf{s}_k|$ between the weight vector and the users' spreading codes, $k = 1, 2, \ldots, 10$, after 2 million transmitted data symbols

4.2 Blindly-Adapted Single-User Detection in Synchronous Systems

One important scenario in which single-user detection can be used is for the mobile unit in a cellular radio system. Assuming that the base station uses a single transmitter for the downlink, all users' signals are synchronous, of equal powers, and with no frequency or phase drifts relative to the desired user's signal; i.e., $P_{rk} = 1$, $\tau_k = 0$, $\Delta\omega_k = 0$, and $\theta_k = 0$, $k = 1, 2, \ldots, K$ (variables as defined in Section 2.1).

Three different sets of randomly generated spreading codes are used, with the purpose of investigating the dependence of the performance on the codes' cross-correlation properties. Since all users' signals are synchronous, the cross-correlation between the desired user's spreading code $\mathbf{s}_1$ and another user's spreading code $\mathbf{s}_k$, $k = 2, 3, \ldots, K$, is given by

$$\varrho_{1,k} = \frac{1}{L}|\mathbf{s}_1^T \cdot \mathbf{s}_k|, \tag{4.8}$$

where L is the length of the filter ($L = 45$), and $\mathbf{s}_1$ and $\mathbf{s}_k$ are vectors of length L, formed by the two spreading waveforms' samples over the spreading waveform repeat period. The absolute value of the cross-correlation is used, because it is a good indicator of the amount of interference created by another user, for all possible combinations of transmitted symbols. The average cross-correlation between the desired user's spreading code and other users' spreading codes in a particular code set is given by

$$\varrho_1 = \frac{1}{K-1}\sum_{k=2}^{K} \varrho_{1,k}, \tag{4.9}$$

where K is the number of users.

The three code sets used in the simulations containing 16 spreading codes each, which is the maximum number of users used in the simulations. For different simulated scenarios the number of users is chosen from the set $K \in \{1, 4, 7, 10, 13, 16\}$. The three code sets are chosen so that the average cross-correlation ϱ_1 is approximately independent of the number of users K for code set 1, and independent of K for code sets 2 and 3. Code set 1 is chosen as a representative of "high-quality" code sets, with a maximum cross-correlation between the desired user's spreading code and another user's spreading code of 0.33 and an average cross-correlation ϱ_1 of 0.11, averaged over different values of K. Code set 2 is a "medium-quality" code set, with

a maximum cross-correlation of 0.47 and an average cross-correlation of 0.2. Finally, code set 3 is a "low-quality" code set, with a maximum cross-correlation of 0.6 and an average cross-correlation of 0.33.

The performance of the CW-FS-LAR adapted using the Griffiths' algorithm and the LCCMA is compared with the fixed-weights case (i.e., the conventional detector) and the case when decision-directed (DD) NLMS adaptation is used after initial adaptation with a training sequence. Figures 4.3, 4.4, 4.5 and 4.6 show the bit-error-rate (BER) performance as a function of the number of users, when code sets 2 and 3 are used, and the pre-despread SNR is -6 dB and -9 dB. In all four cases, it is seen that decision-directed adaptation after training gives the best performance, but that the Griffiths' algorithm and the LCCMA are quite close. The performance of the LCCMA is usually slightly better than that of the Griffiths' algorithm, the difference being larger in cases with more background noise. It is in these cases (Figures 4.5 and 4.6) that the performance of the LCCMA approaches that of decision-directed adaptation after training. In the case of both blind adaptation algorithms the CW-FS-LAR performs much better than the conventional detector, yielding up to two orders of magnitude of difference in BER (Figures 4.3 and 4.4).

For insight into how much the receiver performance depends on the choice of spreading codes, BER curves obtained for the Griffiths' algorithm and the LCCMA using the three different code sets, and for a SNR of -6 dB and -9 dB, are shown in Figures 4.7 and 4.8. Figure 4.9 shows the same curves for the conventional detector. It is seen that in both cases of blind adaptation algorithms the performance of the CW-FS-LAR depends greatly on the choice of spreading codes and their cross-correlation properties. This dependence is considerably greater than in the case of the conventional detector. It is also noticed that there is a lower degree of dependence for higher BER, as seen for the case of $SNR = -9$ dB. Comparing the performance of the Griffiths' algorithm and the LCCMA, it is again concluded that they are very close, but that in most cases the LCCMA performs slightly better than the Griffiths' algorithm.

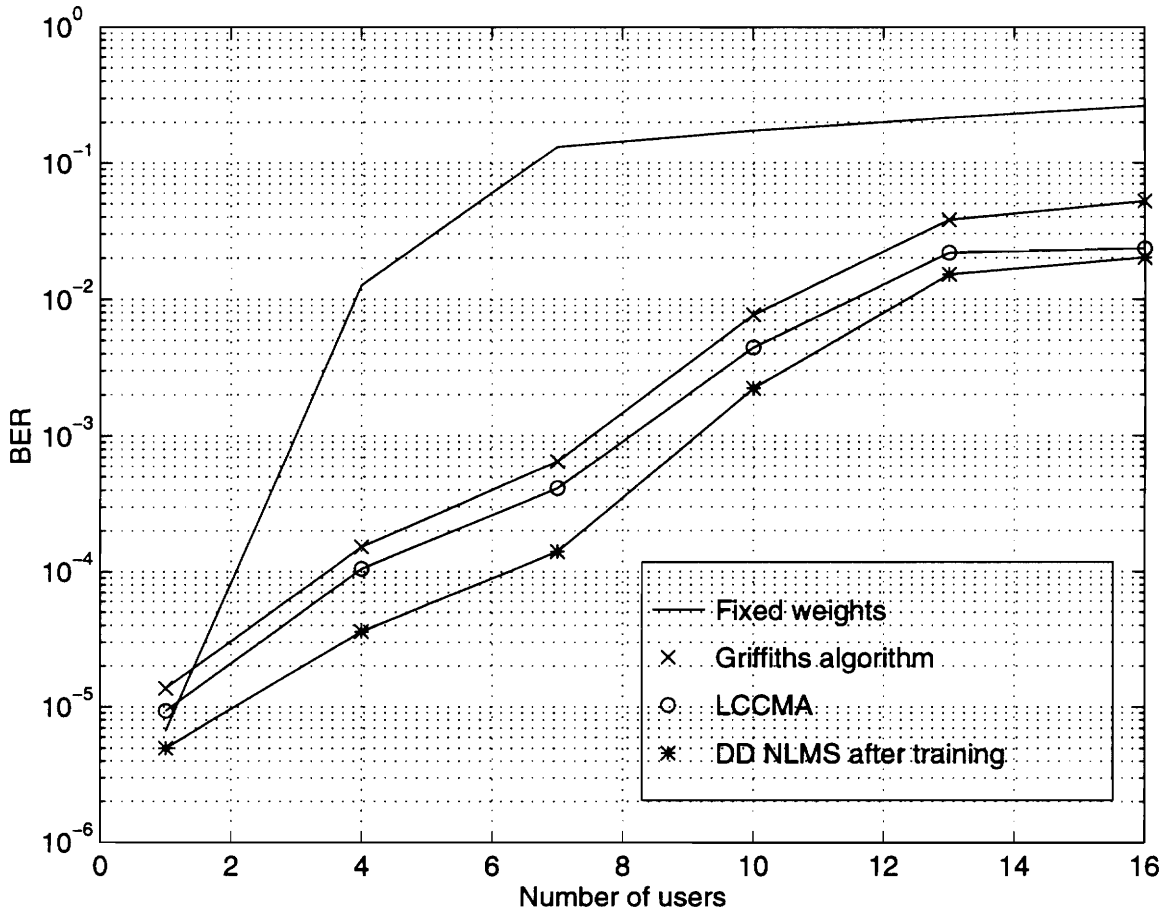

Figure 4.3: Receiver performance in a system with synchronous equal-power signals, for code set 2, and a SNR of -6 dB

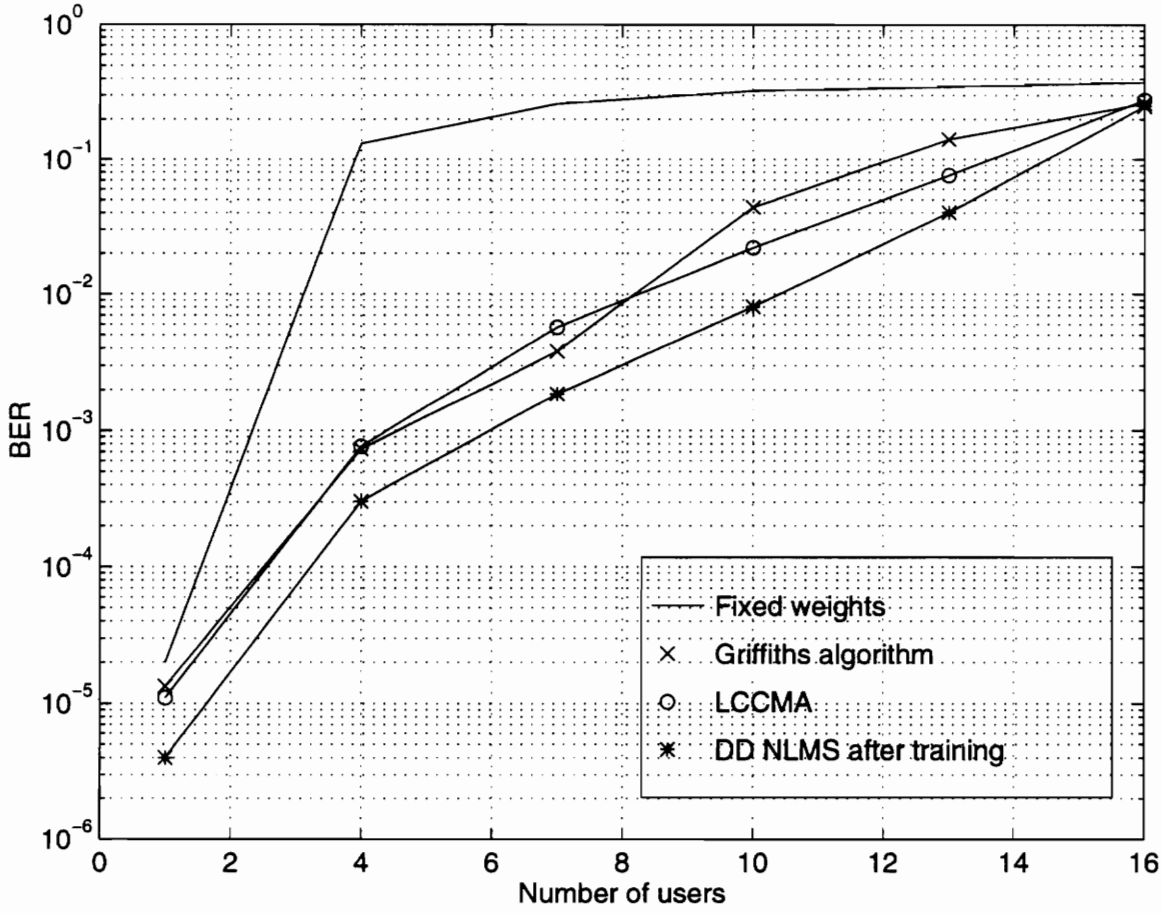

Figure 4.4: Receiver performance in a system with synchronous equal-power signals, for code set 3, and a SNR of -6 dB

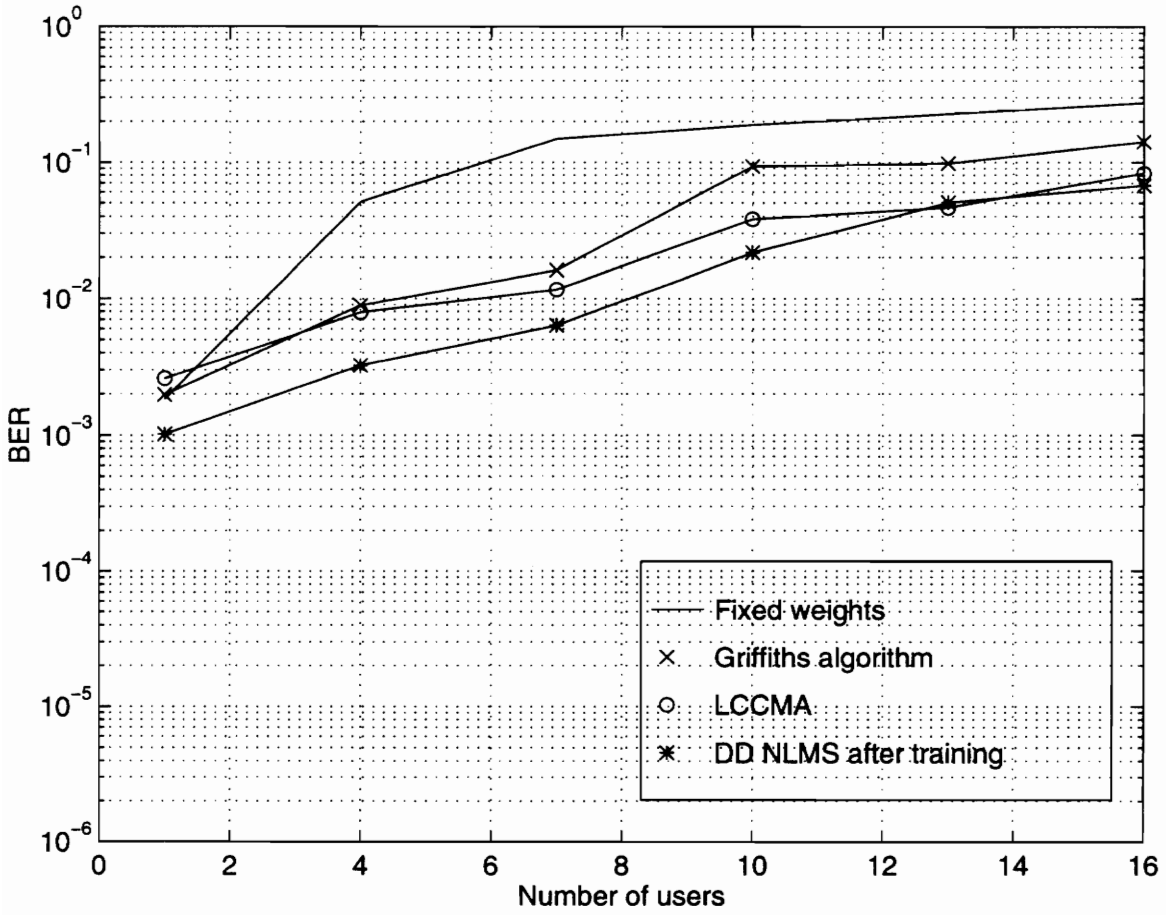

Figure 4.5: Receiver performance in a system with synchronous equal-power signals, for code set 2, and a SNR of -9 dB

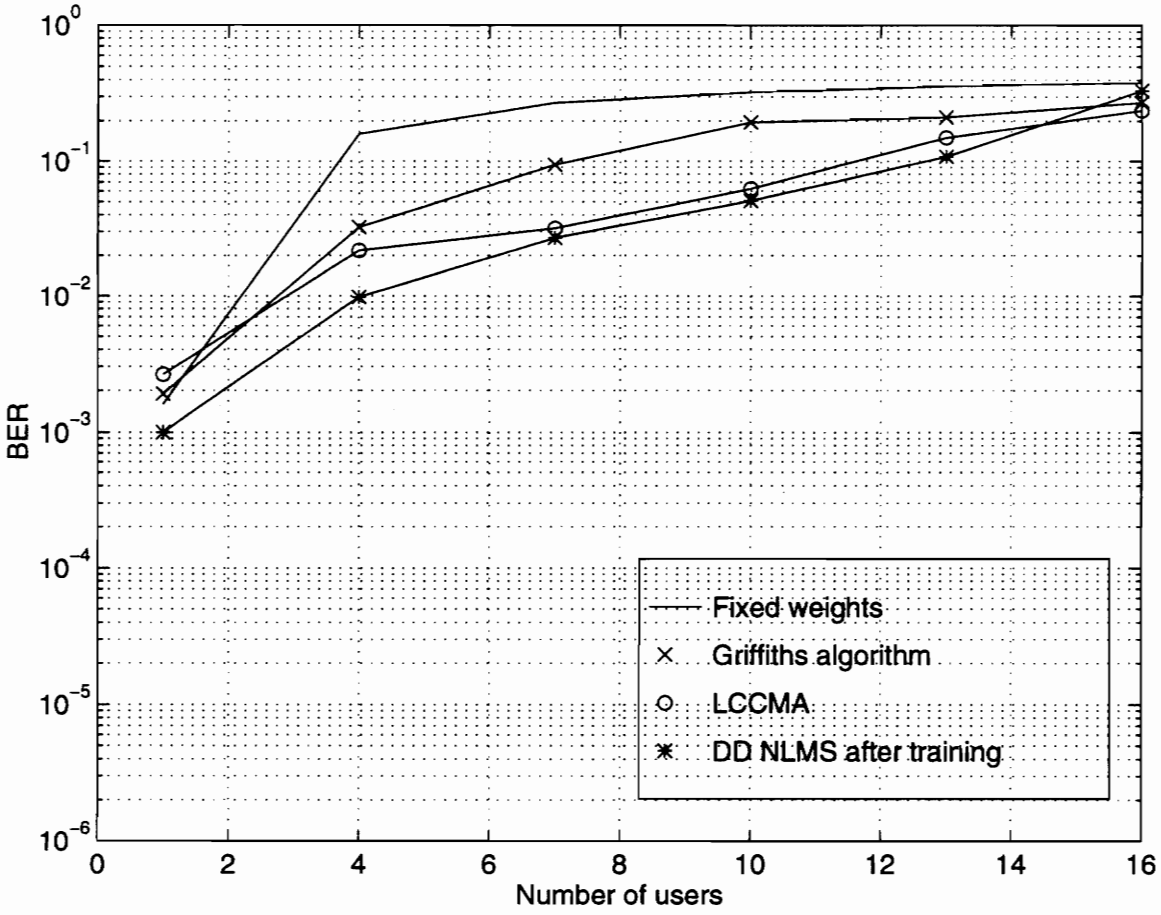

Figure 4.6: Receiver performance in a system with synchronous equal-power signals, for code set 3, and a SNR of -9 dB

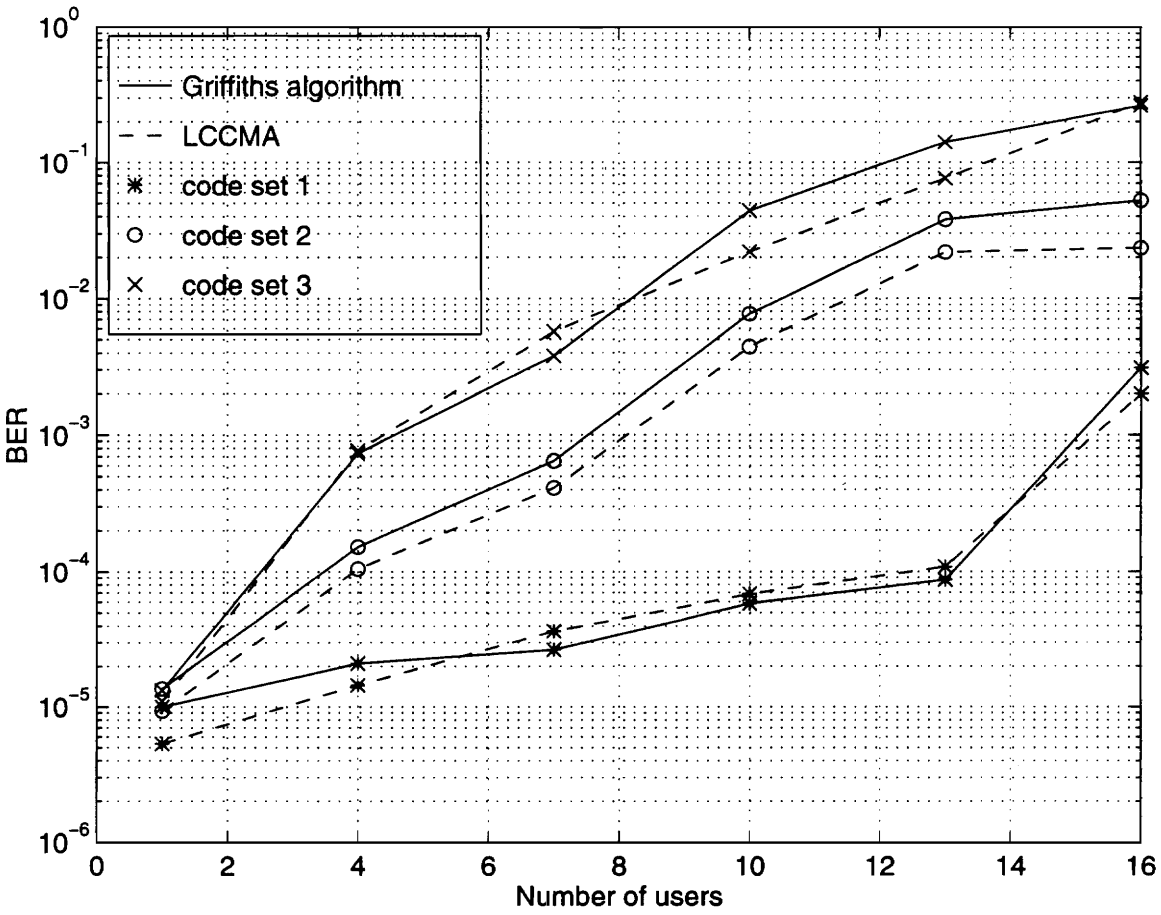

Figure 4.7: Performance of the CW-FS-LAR adapted using the Griffiths' algorithm and the LCCMA in a system with synchronous equal-power signals, for three different code sets, and a SNR of -6 dB

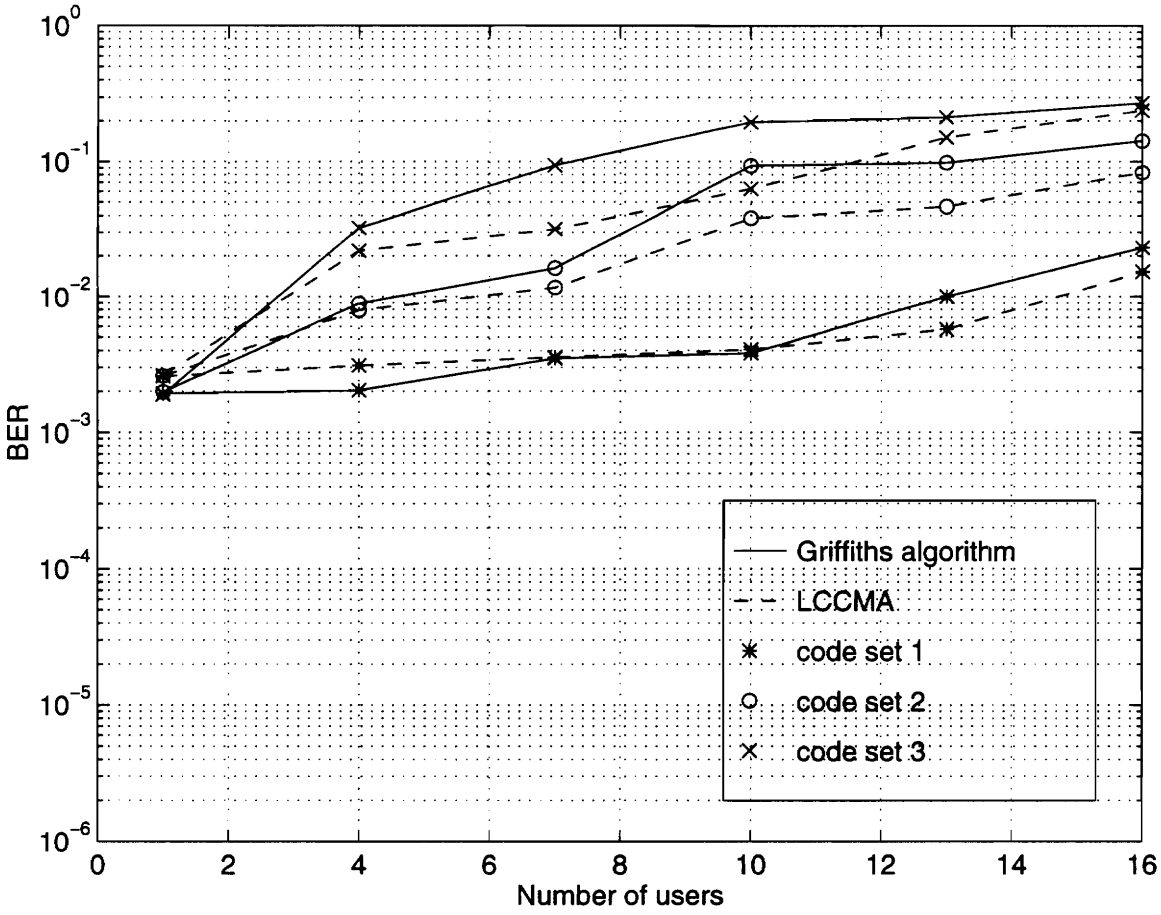

Figure 4.8: Performance of the CW-FS-LAR adapted using the Griffiths' algorithm and the LCCMA in a system with synchronous equal-power signals, for three different code sets, and a SNR of -9 dB

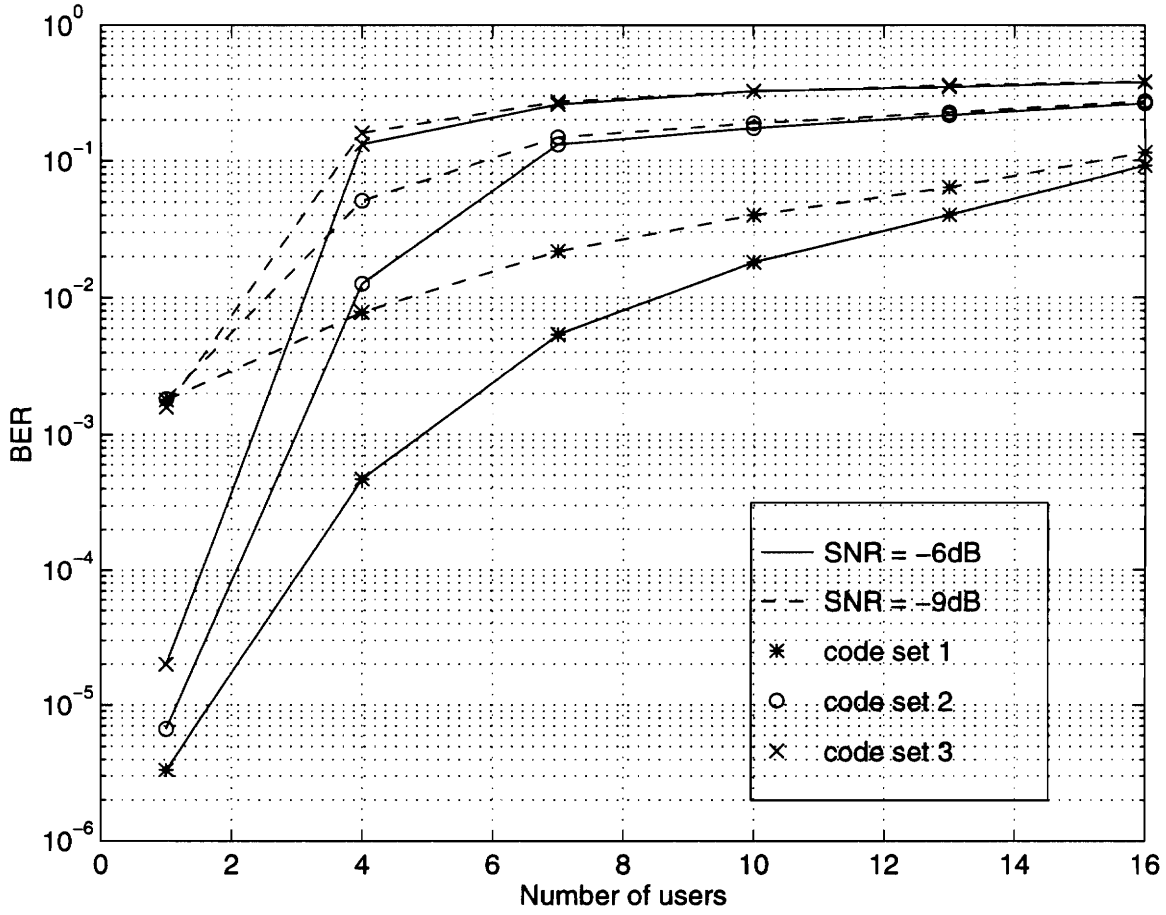

Figure 4.9: Performance of the conventional detector in a system with synchronous equal-power signals, for three different code sets, and a SNR of -6 dB and -9 dB

4.2.1 Convergence Rate of the Blind Adaptation Algorithms Applied to Single-User Detection

In a mobile communications environment fast convergence rate is required so that the adaptation algorithm can track the time-varying channel characteristics and the changing number of users. The convergence rates of the Griffiths' algorithm and the LCCMA are compared to that of the trained NLMS algorithm, the faster converging version of the LMS algorithm.

Figures 4.10 and 4.11 show the mean-squared error (MSE) achieved by the three algorithms in a synchronous system of 7 and 10 users, with a SNR of -6 dB. The LCCMA, unlike the other two algorithms, isn't designed to minimize the MSE, but the CM cost function (Section 3.2.3). However, the MSE is a better indicator of receiver performance, since a low MSE will yield a low BER. When the LCCMA is applied to single-user detection, we are more interested in its convergence in terms of the MSE reaching an approximate steady state providing a low BER. Because the weight vector is linearly constrained so that the receiver captures the desired signal and provides an estimate of the transmitted data symbol at the output, the algorithm tends to minimize the MSE along with the CM cost function (Section 3.2.3). Figures 4.10 and 4.11 show that all three algorithms converge after 500 and 1500 symbols, respectively, and that the misadjustments achieve similar values.

4.2.2 Catastrophic Failure of the Blind Adaptation Algorithms Applied to Single-User Detection

As discussed in Section 3.2, a potential problem for blind adaptation is catastrophic failure. The condition can occur when the signal is severely corrupted by noise and interference and the initial adaptation starts from a "closed eye". In such a case, decision-directed adaptation that uses the fed-back hard data decisions as the reference signal, instead of a training sequence, can fail to converge (Figure 4.12). Instead of being minimized, the MSE grows with each iteration, and the filter output becomes independent of the transmitted desired user's data symbols, i.e., the receiver "fails catastrophically".

It is investigated whether the two blind adaptation algorithms, the Griffiths' algorithm and the LCCMA, suffer from catastrophic failure. A synchronous system is

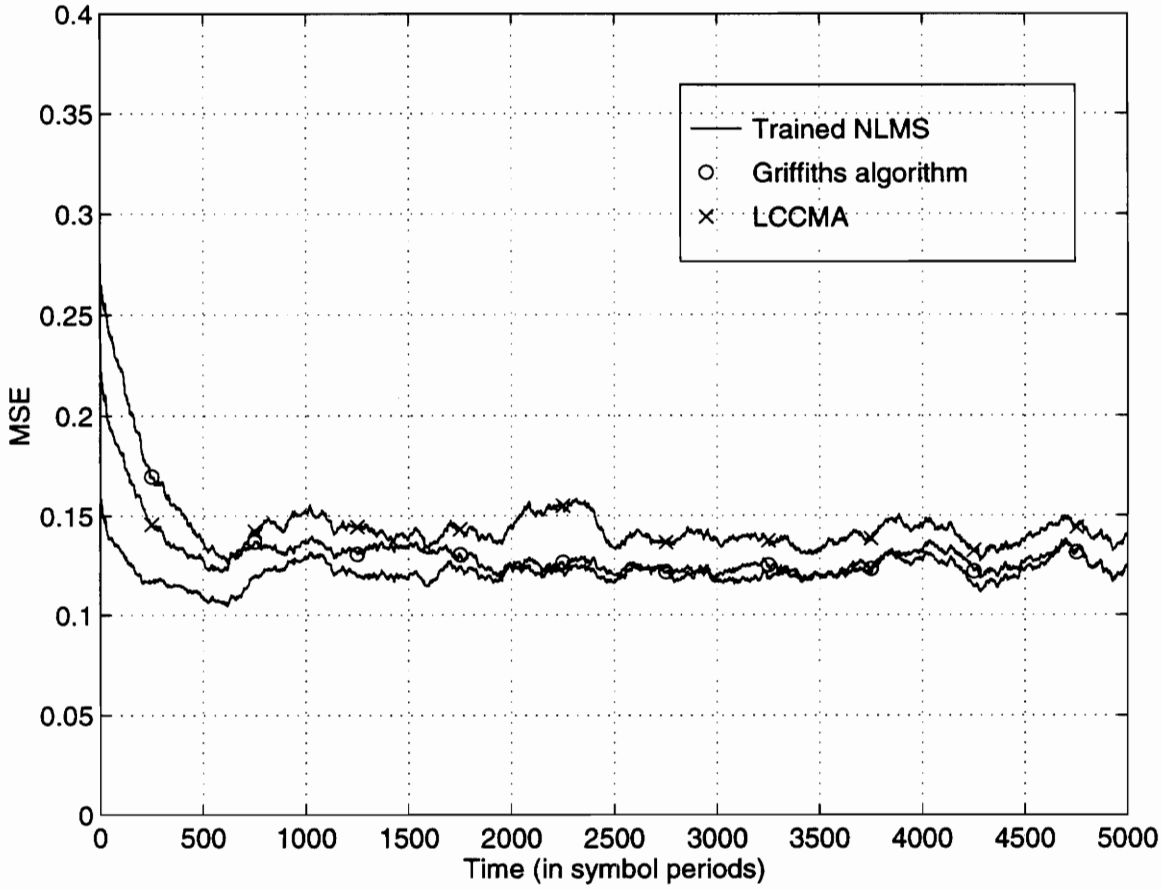

Figure 4.10: Convergance rates in a system with 7 synchronous equal-power signals, for a SNR of -6 dB

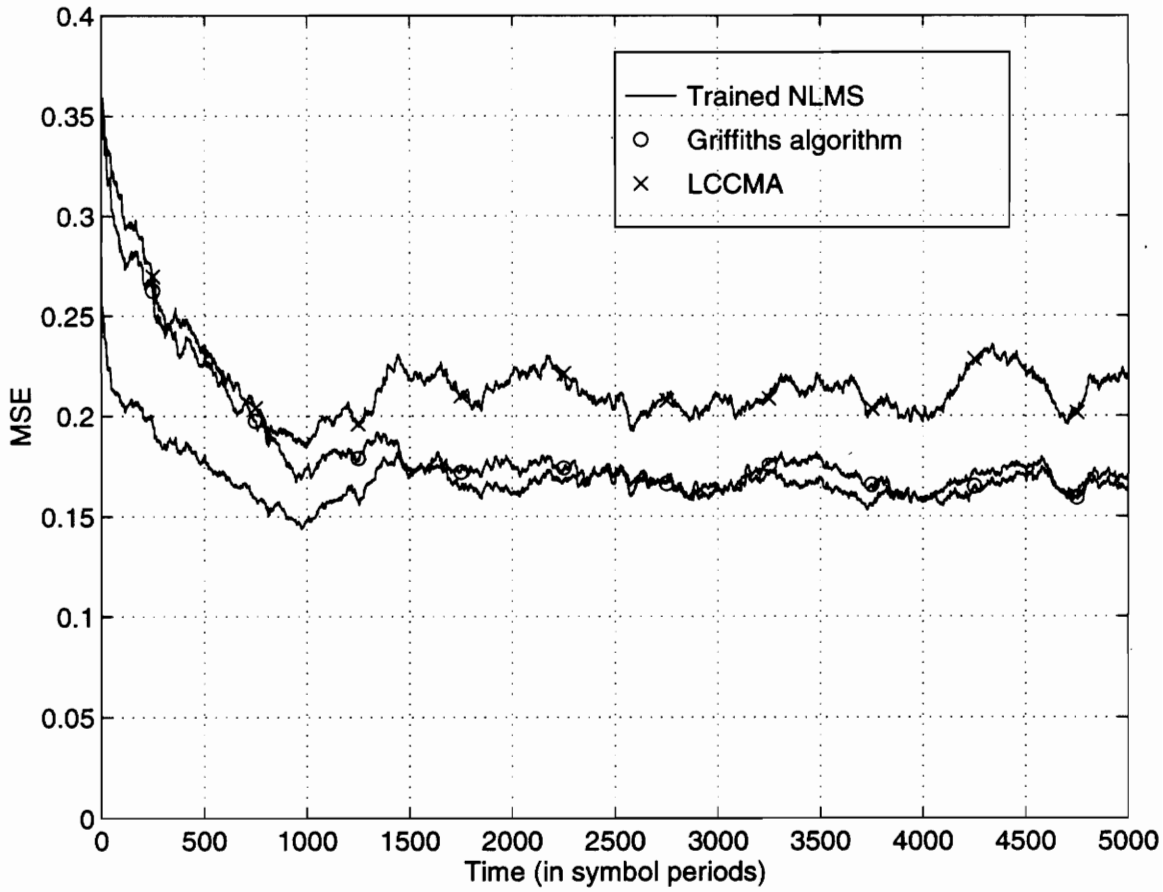

Figure 4.11: Convergance rates in a system with 10 synchronous equal-power signals, for a SNR of -6 dB

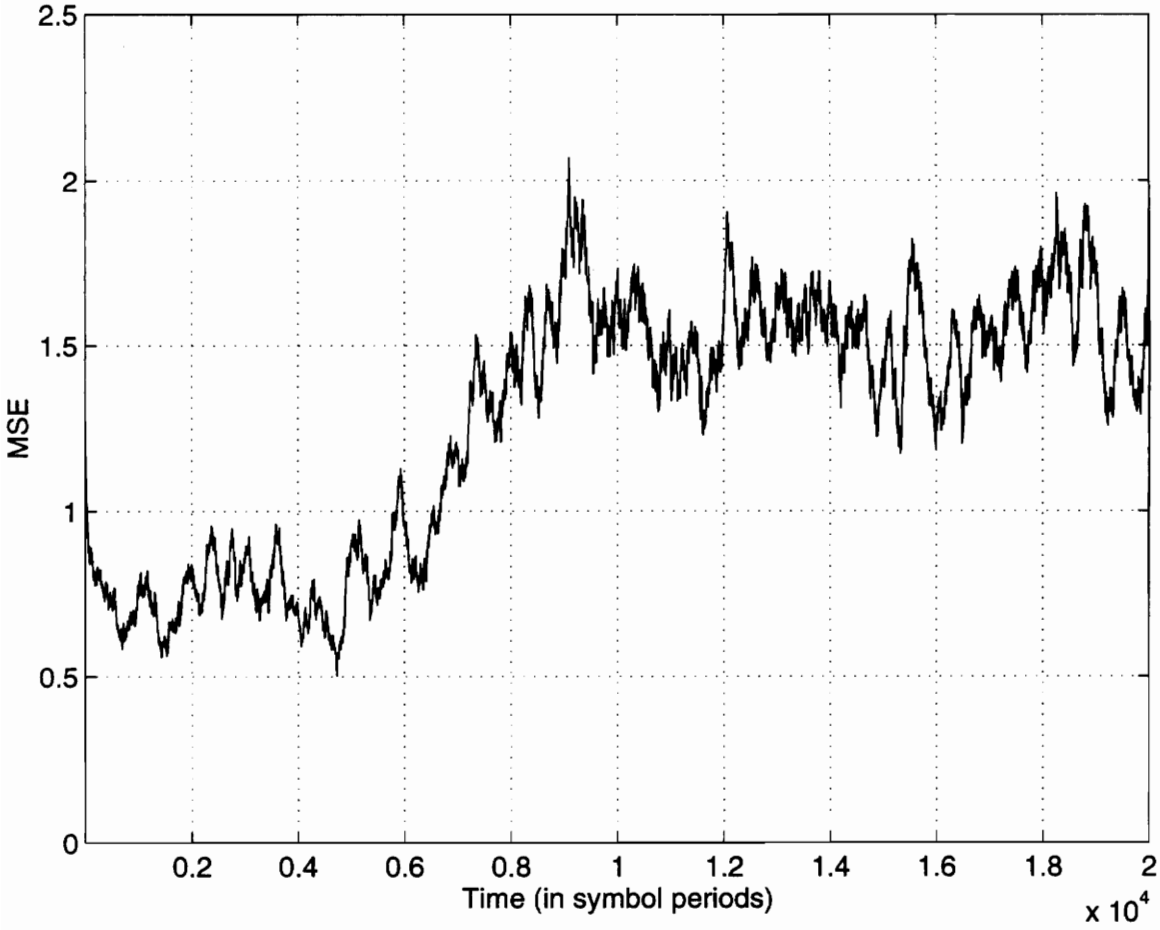

Figure 4.12: Catastrophic failure of decision-directed NLMS adaptation in a synchronous system with 24 users and a SNR of -6 dB

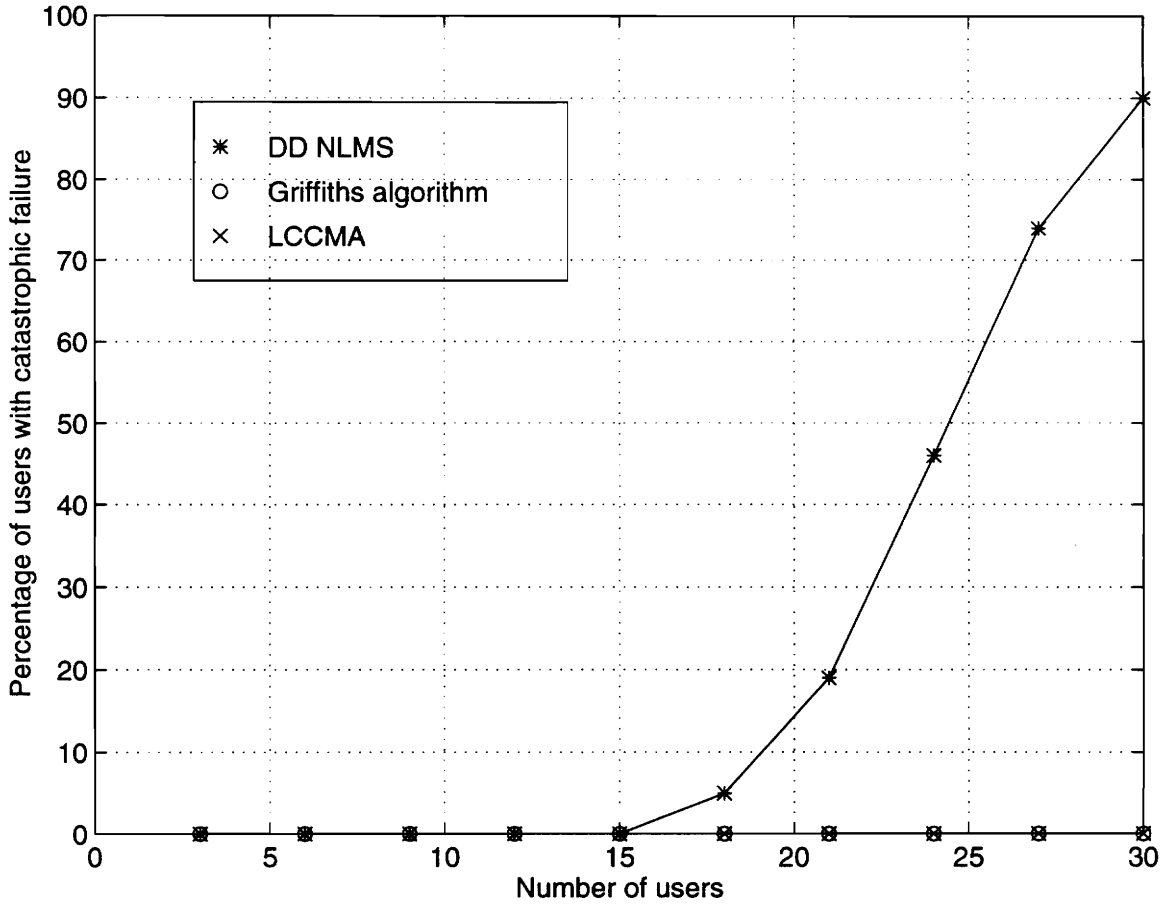

Figure 4.13: Catastrophic failure rates for a synchronous system with a SNR of -6 dB

simulated, with the number of users K varying from 3 to 30, and randomly generated spreading codes. The SNR is -6 dB. Figure 4.13 shows the percentage of users for which the corresponding single-user detectors suffer from catastrophic failure. It is seen that the decision-directed NLMS adaptation suffers from catastrophic failure when the number of users in the system is larger than the processing gain ($N = 15$). As the number of users increases, the rate of catastrophic failure also increases, reaching 90% when the number of users is twice the processing gain. In the case of both the Griffiths' algorithm and the LCCMA, the blind algorithm always converges, and the catastrophic failure rate is equal to zero for all simulated cases.

4.3 Blindly-Adapted Single-User Detection in Asynchronous Systems and the Near-Far Resistance

Assuming that the base station in a cellular radio system uses multiple transmitters for the downlink, instead of a single one, different users' signals can be asynchronous, and can have frequency drifts, phase drifts and varying powers relative to the desired user. This condition is also illustrative of ad-hoc networks. For the simulated system different users' delays relative to the desired user are chosen to be integer multiples of the sampling period (Section 2.1). The frequency offsets are uniformly distributed over the interval [100Hz, 400Hz], and the phase drifts are uniformly distributed over the interval $[0, 2\pi]$. The power variance is chosen to be 1 dB.

Figures 4.14 and 4.15 show the BER curves for the Griffiths' algorithm and the LCCMA, respectively, for the three sets of spreading codes and two values of SNR, -6 dB and -9 dB (BER performance of the conventional receiver in the same system is found in [26]). Each point on the curves is obtained as an average of five simulation runs. It is seen that the performance doesn't depend on the choice of spreading codes, which is expected, considering that the three sets have similar cross-correlation properties when the users in the system are asynchronous.

For the asynchronous system the cross-correlation between the desired user's spreading code and another user's spreading code is given by

$$\varrho_{1,k}(n) = \frac{1}{L}|\mathbf{s}_1^T \cdot \mathbf{s}_k^{(n)}|, \tag{4.10}$$

where n is the delay between the two users in terms of sampling periods, L is the length of the filter ($L = 45$), and $k = 2, 3, \ldots, K$. The two vectors $\mathbf{s}_1$ and $\mathbf{s}_k^{(n)}$ are formed by the corresponding spreading waveforms' samples over the desired symbol period, and are given by

$$\mathbf{s}_1 = \begin{bmatrix} s_{10} & s_{11} & \cdots & s_{1(L-1)} \end{bmatrix}^T \tag{4.11}$$

and

$$\mathbf{s}_k^{(n)} = \begin{bmatrix} s_{kn} & s_{k(n+1)} & \cdots & s_{k(L-1)} & s_{k0} & s_{k1} & \cdots & s_{k(n-1)} \end{bmatrix}^T. \tag{4.12}$$

For code set 1 the maximum cross-correlation defined by (4.10) is 0.6, and the average cross-correlation with the desired user, averaged over all the interferers and delays,

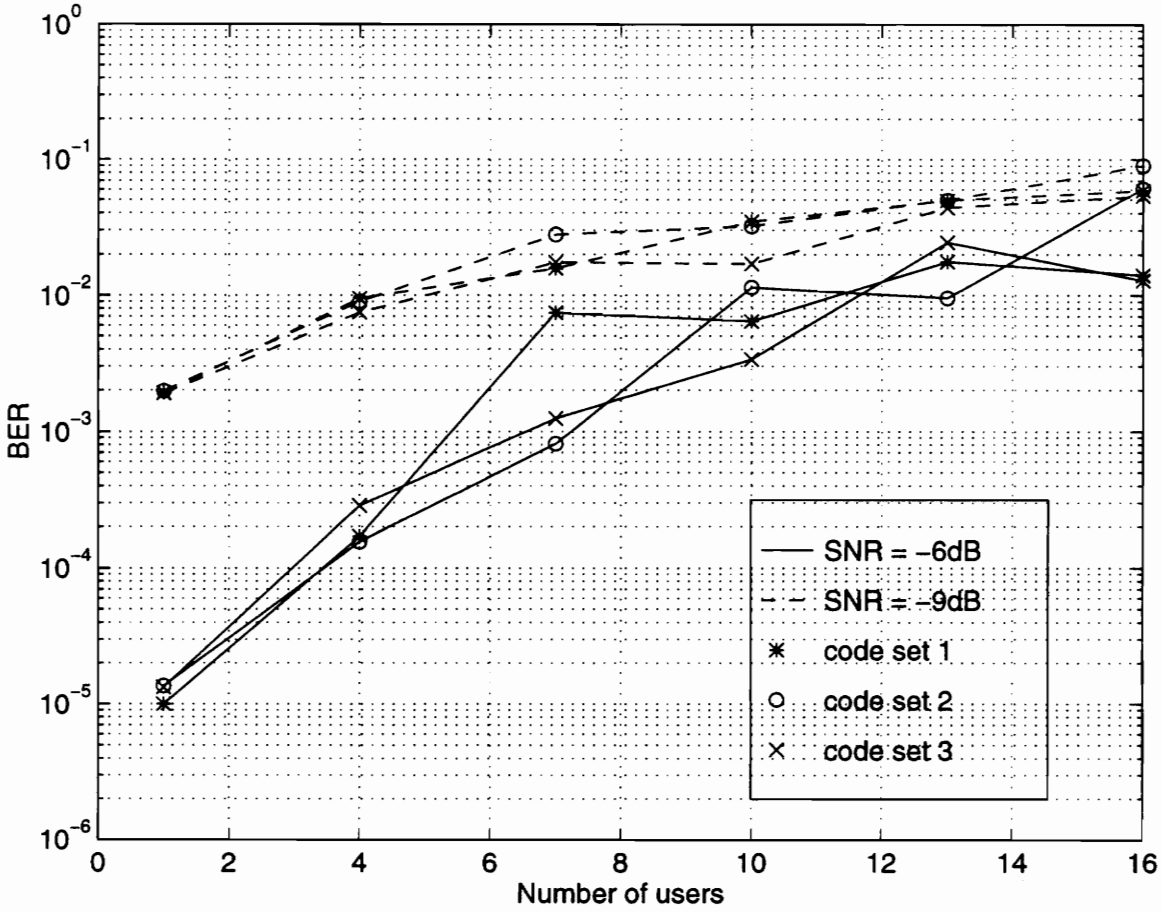

Figure 4.14: Performance of the CW-FS-LAR adapted using the Griffiths' algorithm in an asynchronous system with power variance of 1 dB, for three different code sets, and SNR of -6 dB and -9 dB

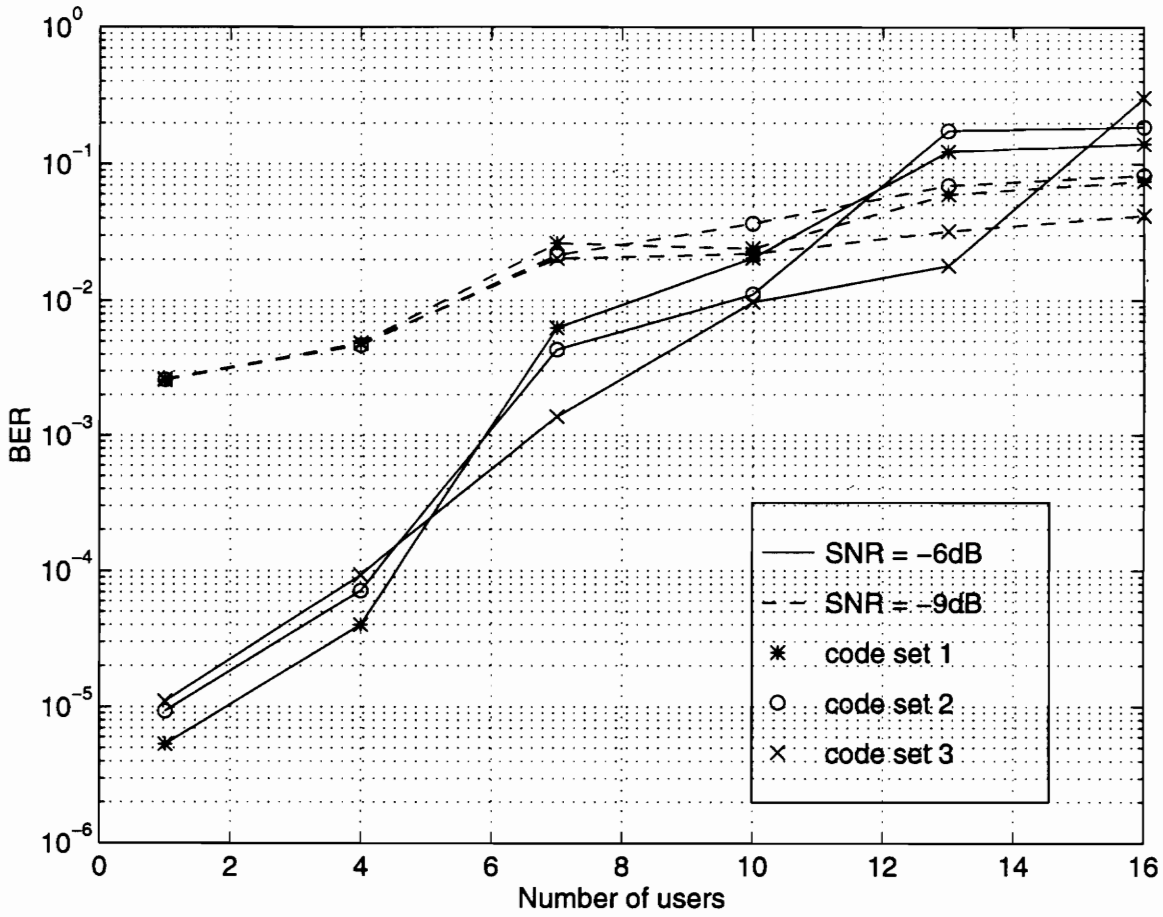

Figure 4.15: Performance of the CW-FS-LAR adapted using the LCCMA in an asynchronous system with power variance of 1 dB, for three different code sets, and SNR of -6 dB and -9 dB

is 0.18. For code set 2 the maximum cross-correlation is 0.73 and the average cross-correlation is 0.2. For code set 3 the maximum cross-correlation is 0.73 and the average cross-correlation is 0.17.

The cross-correlation properties of the three code sets in the asynchronous system are seen to be quite similar. The variations between the BER curves corresponding to different code sets should be contributed more to the random system parameters, such as the power variations and frequency and phase drifts, than to the choice of codes. The curves can thus be used to form a single average curve, which will represent a better estimate of the mean BER, averaged over 15 simulation runs.

Figure 4.16 compares the BER performance of the Griffiths' algorithm and the LCCMA, averaged over the three code sets, for the two values of the SNR. It is seen that the performance of the two algorithms is again very similar, and that the slight advantage of the LCCMA that is observed in the case of a synchronous system is not present in the case of an asynchronous one. Moreover, the LCCMA achieves relatively poor results for the two largest systems (13 and 16 users) and the SNR of -6 dB. This is contributed to outliers among the 15 simulation results, due to particularly unfavorable combinations of random system parameters. More simulation runs are required for a better estimate of the mean BER.

In an ad-hoc wireless network a user would be receiving signals directly from other users instead of a base station, and there would be little or no power control. In order to investigate the possibility of using a blind adaptive receiver in such a network, an asynchronous system with 12 dB power variance and SNR of -6 dB and -9 dB is simulated. The performance of the two blind algorithms in this system, averaged over the three code sets, is compared to that in a system with 1 dB power variance in Figures 4.17 and 4.18. It is seen that there is very little difference in the performance in the two cases of relaxed and strict power control, which shows that the two adaptive receivers are near-far resistant.

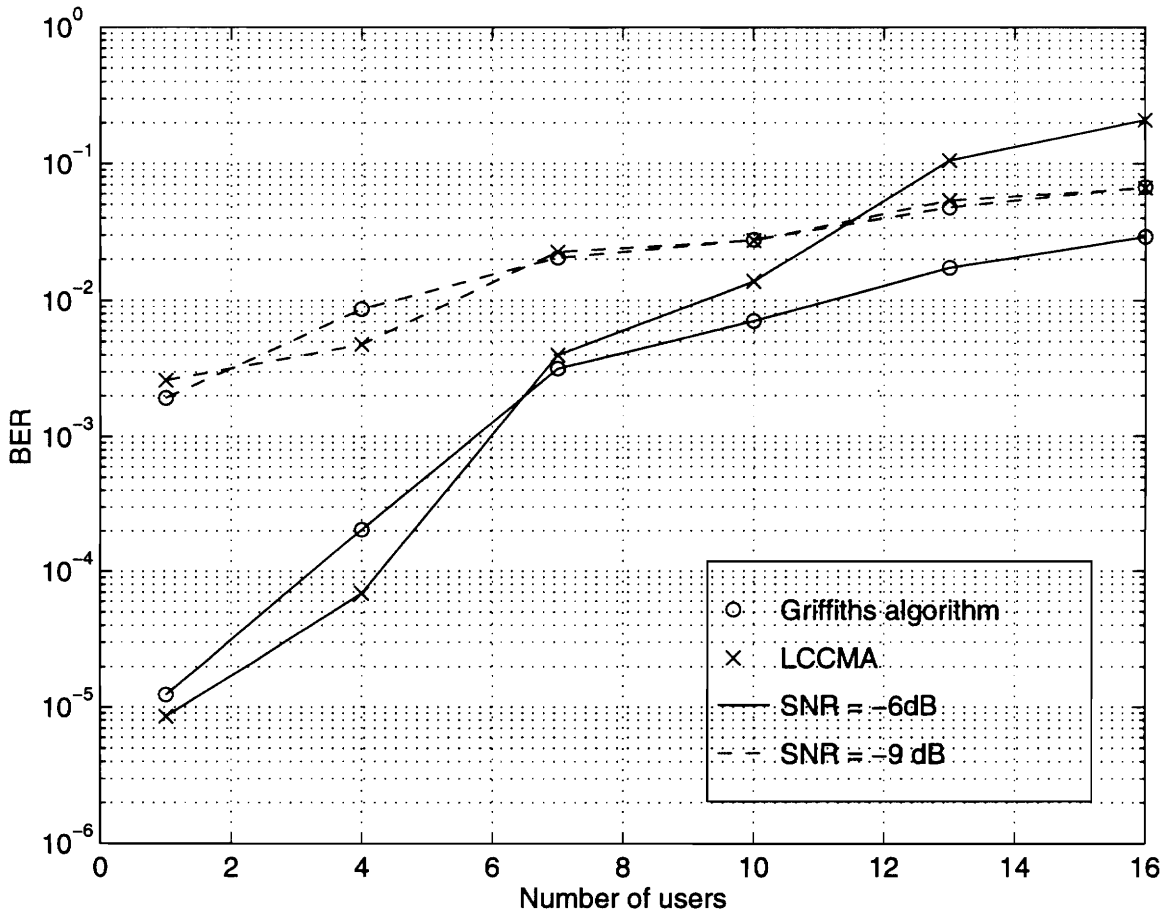

Figure 4.16: Performance of the CW-FS-LAR adapted using the Griffiths' algorithm and the LCCMA in an asynchronous system with power variance of 1 dB, and SNR of -6 dB and -9 dB

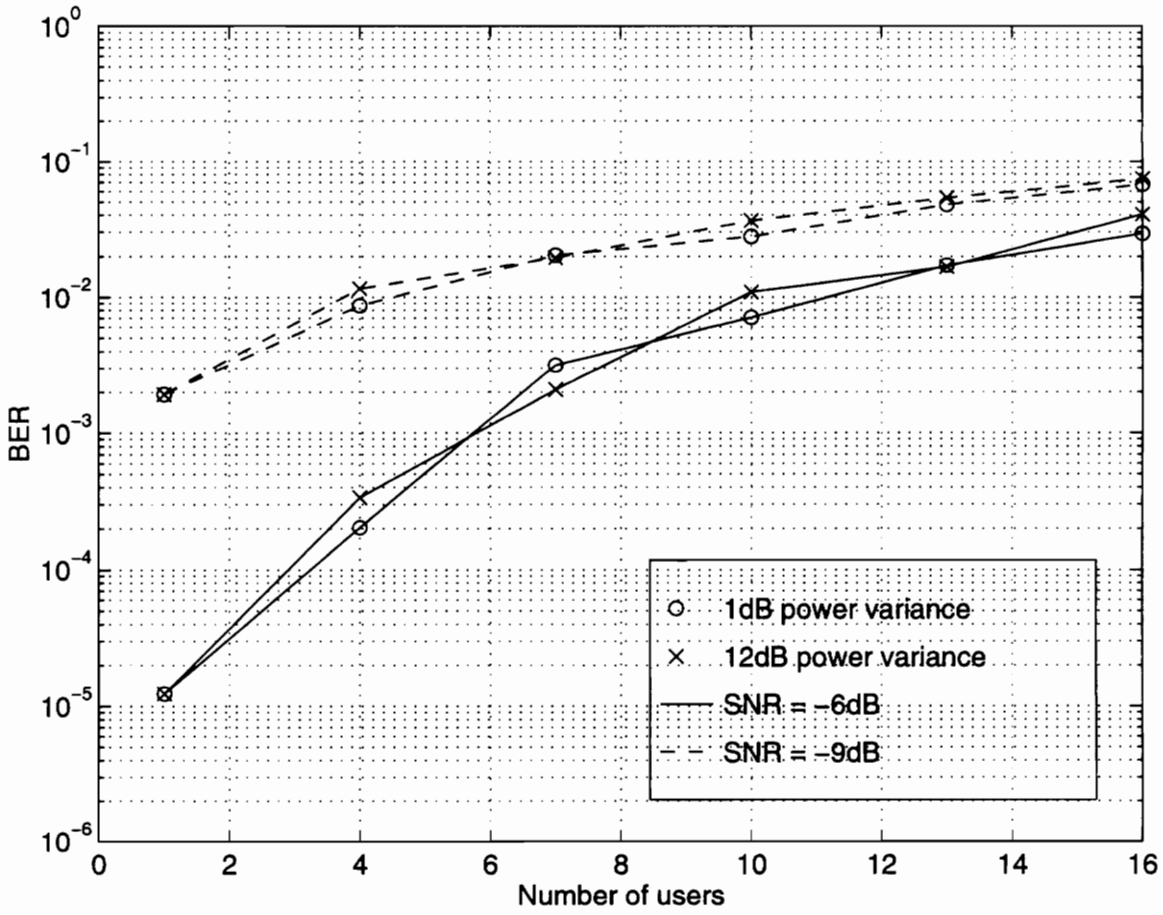

Figure 4.17: Performance of the CW-FS-LAR adapted using the Griffiths' algorithm in an asynchronous system with strict (1 dB power variance) and relaxed (12 dB power variance) power control, and SNR of -6 dB and -9 dB

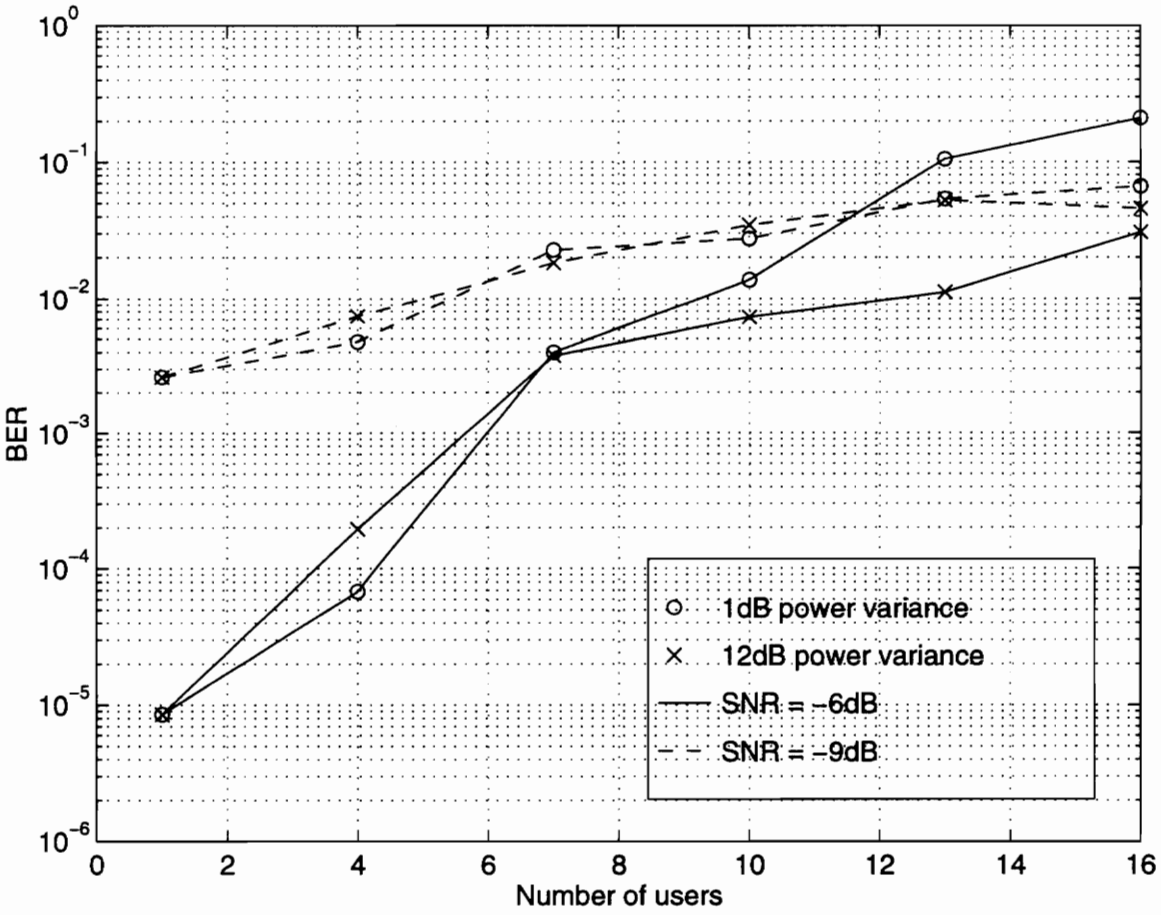

Figure 4.18: Performance of the CW-FS-LAR adapted using the LCCMA in an asynchronous system with strict (1 dB power variance) and relaxed (12 dB power variance) power control, and SNR of -6 dB and -9 dB

Chapter 5

Conclusions

This work concentrated on the area of DSSS-CDMA single-user detection, providing an overview of and discussing a wide range of techniques, and exploring ways for better understanding and improving them.

The reviewed single-user detectors included chip-rate and fractionally-spaced ones, ones with reduced and optimum complexity, and linear and non-linear ones. All of them require only the knowledge of the desired user's spreading code and timing, and have a complexity comparable to that of the conventional receiver.

To give insight into the creation and analysis of different single-user detection techniques, a unifying perspective for single-user detection is presented, contributing to the area. It is shown that for best performance the receiver has to be able to exploit the cyclostationarity inherent to the DSSS-CDMA signal. The analogy with beamforming is also presented. In the frequency domain, the way the receiver despreads the desired user's signal by exploiting spectral correlation is similar to the way an adaptive array exploits spatial diversity when it performs beamforming. In the time domain, the formulation of the desired user's symbol estimation of a DSSS-CDMA single-user detector is shown to be identical to that of a beamformer.

Trained adaptation algorithms commonly used for DSSS-CDMA single-user detection are presented, and requirements for more suitable blind adaptation algorithms are discussed. Three blind adaptation algorithms novel in the area of single-user detection are proposed, making a unique contribution. The algorithms are derived and their complexities discussed. The analogy with beamforming proves particularly useful since all three algorithms are commonly used in that area.

The Griffiths' algorithm was presented in two forms, as the algorithm used for the Applebaum's antenna array, based on the concept of maximizing the SINR, and as a method of steepest descent following the MMSE criterion, when the cross-correlation between the received and the desired signal is known. The algorithm can also be viewed as a modification of the LMS algorithm, which is made blind by making use of the knowledge of the desired user's spreading code.

It was shown that the CMA algorithm, which makes use of the constant modulus property of the desired signal, suffers from the problem of capturing an interferer instead of the desired user, due to the algorithm's inability to distinguish between different constant modulus signals. The LCCMA, an extension to the CMA algorithm, was derived and linear constraints suited to DSSS-CDMA single-user detection proposed, to solve the "capture" problem.

The Griffiths' algorithm and the LCCMA are shown to have complexities larger than that of the LMS. In the case of the Griffiths' algorithm, there is only a slight increase in complexity, whereas in the case of the LCCMA, the complexity increase is more substantial. In both cases, however, the two algorithms have a great advantage over the LMS and NLMS, because they are blind. Both algorithms were shown to converge as fast as the trained NLMS algorithm, and not to suffer from catastrophic failure like the blind decision-directed adaptation.

A single-user detector, namely the CW-FS-LAR, adapted using the two blind adaptation algorithms is shown to yield large gains in system capacity as compared to the conventional detector. In a synchronous system, the BER performance is just slightly worse than in the case of trained adaptation, and it was shown to be greatly dependent on the choice of spreading codes (i.e., their cross-correlation properties). In an asynchronous system, for both blind adaptation methods, the receiver was shown to be near-far resistant, for large disparities in the powers of the MAI.

The performance achieved using the Griffiths' algorithm and the LCCMA was compared. In the case of the synchronous system, the LCCMA was observed to perform slightly better than the Griffiths' algorithm, although not in every single simulated scenario. It should be noted, however, that the Griffiths' algorithm requires less computation and storage, and that the choice of a blind algorithm will depend on this trade-off. In addition to the larger computational and storage requirements, the LCCMA requires estimation of the desired signal's power. This issue was not

addressed in the simulations (the signal power was assumed to be known), and is left for future work. In asynchronous systems, the BER performance achieved using the two blind algorithms is comparable and can be considered to be the same.

Future work in this area should certainly involve simulation of multipath and fading, and investigation of receiver performance under those channel conditions. Also, the convergence rate of the two blind adaptation algorithms should be investigated for varying channel characteristics and system parameters, to see how well the algorithms track the changes. It should be noted that certain modifications to the single-user detector and the adaptation procedure will have to be made in these cases. The length of the adaptive filter should be increased, so that the delay spread affecting the symbol period is taken into account. It should correspond to the duration of the whole spread and by multipath modified desired user's symbol. Also, the effect that the channel has on the desired user's spreading waveform should be taken into account. The desired user's spreading code, which figures in both blind adaptation algorithms, should in this case be replaced by the sum of scaled and delayed versions of the spreading code, formed by the multipath. This means that the channel will need to be estimated with some required minimum degree of accuracy.

The dependence of the receiver performance on the choice of spreading codes, which was seen to be greater than in the case of conventional detection, should also be investigated. The performance will be greatly improved if mechanisms for generating a large number of low-cross-correlation spreading codes are devised.

Bibliography

[1] R. L. Pickholtz, D. L. Schilling, L. B. Milstein, "Theory of Spread Spectrum Communications–A Tutorial," *IEEE Transactions on Communications*, Vol. COM–30, No. 5, pp. 855–884, May 1982.

[2] S. Verdú, "Adaptive Multiuser Detection," *Proc. IEEE 3rd International Symposium on Spread Spectrum Techniques and Applications*, Vol. 1, pp. 43–50, 1994.

[3] A. Duel-Hallen, J. Holtzman, Z. Zvonar, "Multiuser Detection for CDMA Systems," *IEEE Personal Communications*, pp. 46–58, April 1995.

[4] S. Verdú, "Minimum Probability of Error for Asynchronous Gaussian Multiple-Access Channels," *IEEE Transactions on Information Theory*, Vol. IT–32, No. 1, pp. 85–96, January 1986.

[5] U. Madhow, M. L. Honig, "Minimum Mean Squared Error Interference Suppression for Direct-Sequence Spread-Spectrum Code-Division Multiple-Access," *Proc. 1st Int. Conf. Universal Personal Commun.*, Dallas, TX, Sept. 28–Oct. 1, pp. 273–277, 1992.

[6] U. Madhow, M. L. Honig, "Error Probability and Near-far Resistance of Minimum Mean Squared Error Interference Suppression Schemes for CDMA," *Proc. IEEE GLOBECOM*, pp. 1339–1343, 1992.

[7] U. Madhow, M. L. Honig, "MMSE Interference Suppression for Direct-Sequence Spread-Spectrum CDMA," *IEEE Transactions on Communications*, Vol. 42, No. 12, pp. 1339–1343, December 1994.

[8] B. G. Agee, "Solving the Near-Far Problem: Exploitation of Spatial and Spectral Diversity in Wireless Personal Communication Networks," *Virginia Tech's Third Symposium on Wireless Personal Communications*, pp. 9–11, June 1993.

[9] E. G. Ström, S. L. Miller, "Optimum Complexity Reduction of Minimum Mean Square Error DS-CDMA Receivers," *IEEE Vehicular Technology Conference*, pp. 568–571, 1994.

[10] P. Monogioudis, R. Tafazolli, B. G. Evans, "LFSE Interference Cancellation in CDMA Systems," *IEEE International Conference on Communications*, pp. 1160–1163, 1994.

[11] P. Monogioudis, R. Tafazolli, B. G. Evans, "Autonomous CDMA Multipath Diversity Receiver," *Proc. IEEE 3rd International Symposium on Spread Spectrum Techniques and Applications*, Vol. 2, pp. 430–434, 1994.

[12] P. B. Rapajić, B. S. Vučetić, "Adaptive Receiver Structures for Asynchronous CDMA Systems," *IEEE Journal on Selected Areas in Communications*, Vol. 12, No. 4, pp. 685–697, 1994.

[13] V. Aue, J. H. Reed, "An Interference Robust CDMA Demodulator that Uses Spectral Correlation Properties," *IEEE Vehicular Technology Conference*, pp. 563–567, 1994.

[14] V. Aue, "Optimum Linear Single User Detection in Direct-Sequence Spread-Spectrum Multiple Access Systems," Master's Thesis, Virginia Polytechnic Institute and State University, February 1994.

[15] R. D. Holley, J. H. Reed, "Time Dependent Adaptive Filters for Interference Cancellation in CDMA Systems," Workshop on Cyclostationary Signal Processing, Monterey, California, August 1994.

[16] R. D. Holley, "Time Dependent Adaptive Filters for Interference Cancellation in CDMA Systems," Master's thesis, Virginia Polytechnic Institute and State University, September 1993.

[17] M. Abdulrahman, D. D. Falconer, A. U. H. Sheikh, "Equalization for Interference Cancellation in Spread Spectrum Multiple Access Systems," *IEEE Vehicular Technology Conference*, pp. 71–74, 1992.

[18] M. Abdulrahman, A. U. H. Sheikh, D. D. Falconer, "DFE Convergence for Interference Cancellation in Spread Spectrum Multiple Access Systems," *IEEE Vehicular Technology Conference*, pp. 807–810, 1993.

[19] M. Abdulrahman, A. U. H. Sheikh, D. D. Falconer, "Decision Feedback Equalization for CDMA in Indoor Wireless Communications," *IEEE Journal on Selected Areas in Communications*, Vol. 12, No. 4, pp. 698–706, May 1994.

[20] R. D. Gitlin, S. B. Weinstein, "Fractionally-Spaced Equalization: An Improved Digital Transversal Equalizer," *The Bell System Technical Journal*, Vol. 60, No. 2, pp. 275–296, February 1981.

[21] J. H. Reed, T. C. Hsia, "The Performance of Time-Dependent Adaptive Filters for Interference Rejection," *IEEE Transactions on Acoustics, Speech and Signal Processing*, Vol. 38, No. 8, pp. 1373–1385, August 1990.

[22] W. A. Gardner, "Cyclic Wiener Filtering: Theory and Method," *IEEE Transactions on Communications*, Vol. 41, No. 1, pp. 151–163, January 1993.

[23] J. H. Reed, C. D. Greene, T. C. Hsia, "Demodulation of a Direct Sequence Spread-Spectrum Signal Using an Optimal Time-Dependent Receiver," *1989 Military Communications Conference*, pp. 657–662, 1989.

[24] B. D. Van Veen, K. M. Buckley, "Beamforming: A Versatile Approach to Spatial Filtering," *IEEE ASSP Magazine*, pp. 4–24, 1988.

[25] R. T. Compton, *Adaptive Antennas: Concepts and Performance*, Prentice Hall, New Jersey, 1988.

[26] M. Majmundar, "Adaptive Single-User Receivers for Direct-Sequence CDMA Systems," Master's thesis, Virginia Polytechnic Institute and State University, April 1996.

[27] B. Widrow, P. E. Mantey, L. J. Griffiths, B. B. Goode, "Adaptive Antenna Systems," *Proceedings of the IEEE*, Vol. 55, No. 12, pp. 2143–2159, December 1967.

[28] B. Widrow, S. D. Stern, *Adaptive Signal Processing*, Prentice Hall, 1985.

[29] S. Haykin, *Adaptive Filter Theory*, 2nd edition, Prentice Hall, New Jersey, 1991.

[30] J. R. Treichler, C. R. Johnson, Jr., M. G. Larimore, *Theory and Design of Adaptive Filters,* John Wiley & Sons, 1987.

[31] E. Nicolau, D. Zaharia, *Adaptive Arrays*, Elsevier Science Publication Company, 1989.

[32] J. R. Treichler, "Adaptive Algorithms that Restore Signal Properties," *IEEE Proceedings of the Int. Conf. on ASSP*, 1984.

[33] J. R. Treichler, B. G. Agee, "A New Approach to Multipath Correction of Constant Modulus Signals," *IEEE Transactions on ASSP*, Vol. ASSP-31, No. 2, pp. 459–471, April 1983.

[34] J. R. Treichler, M. G. Larimore, "CMA-based Techniques for Adaptive Interference Rejection," *1986 Military Communications Conference*, 1986.

[35] R. Gooch, J. Lundell, "The CM Array: An Adaptive Beamformer for Constant Modulus Signals," *Proceedings of the Int. Conf. on ASSP*, pp. 2523–2526, Tokyo, Japan, April 1986.

[36] M. J. Rude, L. J. Griffiths, "Incorporation of Linear Constraints into the Constant Modulus Algorithm," *IEEE Proceedings of the Int. Conf. on ASSP*, pp. 968–971, 1989.

[37] M. J. Rude, L. J. Griffiths, "An Untrained, Fractionally-Spaced Equalizer for Co-Channel Interference Environments," *24th Asilomar Conference on Signals, Systems and Computers*, 1990.

[38] M. J. Rude, L. J. Griffiths, "A Linearly Constrained Adaptive Algorithm for Constant Modulus Signal Processing," *Signal Processing V: Theories and Applications*, edited by L. Torres at al., Elsevier Science Publishers B. V., 1990.

[39] M. L. Honig, U. Madhow, S. Verdú, "Blind Adaptive Interference Suppression for Near-Far Resistant CDMA," *Proc. IEEE GLOBECOM*, pp. 379–384, December 1994.

[40] N. Zečević, M. Majmundar, J. H. Reed, "Interference Rejection Techniques for Direct-Sequence Spread-Spectrum CDMA Single-User Detection: A Comparative Study," in preparation

[41] R. Lupas, S. Verdú, "Linear Multiuser Detectors for Synchronous Code-division Multiple-Access Channels," *IEEE Trans. Inform. Theory*, Vol. IT–35, No. 1, pp. 123–136, January 1989.

Vita

Nevena Zečević was born in Niš, Yugoslavia, on August 19, 1969. She received a B.S.Eng. degree in electronics and communications from the Department of Electrical Engineering of the University of Belgrade, Yugoslavia, in 1993. The topic of her undergraduate thesis was "A Modified Viterbi Decoder with a Reduced Number of Possible Paths". The main interest of her graduate studies was in the area of communications, especially wireless and digital communications. She joined the Mobile and Portable Radio Research Group (MPRG) in May 1994, where she worked as a Graduate Research Assistant from October 1994 until December 1995. She presently works as a Systems Engineer in Motorola, Inc., in Fort Worth, Texas. Her main interests are in the areas of wireless and digital communication systems design and digital signal processing.